

1 Drivers of Phytoplankton Bloom Interannual Variability in the Amundsen and Pine 2 Island Polynyas

3
4 Guillaume Liniger^{1,2*}, Delphine Lannuzel^{1,3,4}, Sébastien Moreau^{5,6}, Michael S. Dinniman⁷,
5 Peter G. Strutton^{1,3}

6 ¹ Institute for Marine and Antarctic Studies, University of Tasmania, Hobart, Australia

7 ² Monterey Bay Aquarium Research Institute, Moss Landing, CA, USA

8 ³ Australian Centre for Excellence in Antarctic Science, University of Tasmania, Hobart,
9 Australia

10 ⁴ Australian Antarctic Program Partnership, University of Tasmania, Hobart, Australia

11 ⁵ Norwegian Polar Institute, Tromsø, Norway

12 ⁶ iC3: Centre for ice, Cryosphere, Carbon and Climate, Department of Geosciences, UiT The
13 Arctic University of Norway, 9037 Tromsø, Norway

14 ⁷ Center for Coastal Physical Oceanography, Old Dominion University, Norfolk, VA, USA

15
16 * Corresponding Author: Guillaume Liniger (liniger@mbari.org)

18 Abstract

19 The Amundsen Sea Embayment (ASE) experiences both the highest ice shelf melt rates and the
20 highest biological productivity in West Antarctica. Using 19 years of satellite data and modelling
21 output, we investigate the long-term influence of environmental factors on the phytoplankton
22 bloom in the Amundsen Sea (ASP) and Pine Island polynyas (PIP). We test the prevailing
23 hypothesis that changes in ice shelf melt rate could drive interannual variability in the polynyas'
24 surface chlorophyll-*a* (chl*a*) and Net Primary Productivity (NPP). We find that the interannual
25 variability and long-term change in glacial meltwater may play an important role in chl*a* variance
26 in the ASP, but not for NPP. Glacial meltwater does not explain the variability in both chl*a* and
27 NPP in the PIP, where light and temperature are the main drivers. We attribute this to potentially
28 greater amount of iron-enriched meltwater brought to the surface by the meltwater pump

Style Definition: Bibliography: Indent: Before: 0 cm,
First line: 0 cm, Space After: 12 pt, Line spacing: single

Deleted: ³

Deleted: ⁵,

Deleted: Moreau^{6,7}

Deleted: Dinniman⁸

Formatted: Not Superscript/ Subscript

Deleted: ^{2,4}

Deleted: ² Australian Research Council Centre of Excellence
for Climate Extremes, University of Tasmania, Hobart,
Australia¹
3...

Deleted: ⁴

Deleted: ⁵

Deleted: ⁶

Deleted: ⁷

Deleted: ⁸

Deleted: investigated

Deleted: sea

Deleted: tested

Deleted: found

47 downstream of the PIP, and the coastal ocean circulation accumulating and transporting iron
48 towards the ASP.

49

50 **Short Summary**

51 We investigate the phytoplankton bloom variability and its drivers in the Amundsen polynyas
52 (areas of open water within sea ice). Between 1998 and 2017, we find that changes in melting ice
53 shelves may have different impacts on biological productivity between the Amundsen Sea (ASP)
54 and Pine Island (PIP) polynyas. While ice shelves melting seems to play an important role for
55 phytoplankton growth variability in the ASP, light and warmer waters appear to be more
56 important in the PIP.

57

58 1. Introduction

59
60 Coastal polynyas are open ocean areas formed by strong katabatic winds pushing sea ice offshore
61 (Morales Maqueda, 2004). They are the most biologically productive areas in the Southern
62 Ocean (SO) relative to their size (Arrigo et al., 1998). This high biological productivity contrasts
63 sharply with the rest of the SO, where low iron and light availability generally co-limit
64 phytoplankton growth (Boyd et al., 2007). In West Antarctica, the Amundsen Sea Embayment
65 (ASE) hosts two of the most productive Antarctic polynyas: The Pine Island Polynya (PIP) and
66 Amundsen Sea Polynya (ASP) (Arrigo and van Dijken, 2003).

67

68 The phytoplankton community in the ASE is generally dominated by *Phaeocystis antarctica*
69 (Lee et al., 2017; Yager et al., 2016), which is adapted to low iron availability and variable light
70 conditions, and forms large summer blooms (Alderkamp et al., 2012; Yager et al., 2016).
71 Diatoms like *Fragilariopsis sp.* and *Chaetoceros sp.* are also present, often becoming more
72 important near the sea-ice edge or under shallow, stratified mixed layers where silicic acid (Si)
73 and iron (Fe) are more available (Mills et al., 2012). In exceptional years, such as 2020, diatoms
74 like *Dactyliosolen tenuijunctus* replaced *P. antarctica* as the dominant taxon, driven by
75 anomalously shallow mixed layers and sufficient Fe–Si supply (Lee et al., 2022). This dynamic
76 balance highlights how light, nutrient supply, and stratification control community composition
77 in these highly productive and complex Antarctic systems.

Deleted: Our study investigates the links between
Deleted: environmental parameters
Formatted: Font color: Auto, Pattern: Clear
Formatted: Font color: Auto, Pattern: Clear
Formatted: Font color: Auto, Pattern: Clear
Deleted: Pine Island (PIP) and
Formatted: Font color: Auto, Pattern: Clear
Deleted: shelf
Formatted: Font color: Auto, Pattern: Clear
Formatted: Font color: Auto, Pattern: Clear
Deleted: ... [1]

1275
1276 The ASE is also the Antarctic region experiencing the highest mass loss from the Antarctic ice
1277 sheet. It has been undergoing increased calving, melting, thinning and retreat over the past three
1278 decades (Paolo et al., 2015; Rignot et al., 2013; Rignot et al., 2019; Shepherd et al., 2018). In the
1279 ASE, this ice loss is mainly through enhanced basal melting of the ice shelves. This is attributed
1280 to an increase in wind-driven Circumpolar Deep Water (CDW) fluxes and ocean heat content
1281 intruding onto the continental shelf through deep troughs such as the Pine Island and Dotson-
1282 Getz, and flowing into the ice shelves cavities (Dotto et al., 2019; Jacobs et al., 2011; Pritchard et
1283 al., 2012). There, warm waters fuel intense basal melt of the Pine Island, Thwaites, and Getz ice
1284 shelves, and returns as a fresher, colder outflow that can strengthen stratification (Jenkins et al.,
1285 2010; Ha et al., 2014). The PIP and ASP differ in their exposure to CDW and in local
1286 circulation: the ASP is more strongly influenced by upwelled modified CDW (mCDW) and
1287 glacial meltwater inputs, whereas in the PIP, vertical intrusions primarily occur beneath the ice
1288 shelves, leading to a more stratified and less directly ventilated surface layer (Assmann et al.,
1289 2013; Dutrieux et al., 2014). These hydrographic contrasts can shape the timing and magnitude
1290 of phytoplankton blooms and nutrient dynamics across the two polynyas.

1291
1292 Melting ice shelves can explain about 60% of the biomass variance between all Antarctic
1293 polynyas, suggesting that they are the primary supplier of dissolved iron (dFe) to coastal
1294 polynyas (Arrigo et al., 2015), and can directly or indirectly contribute to regional marine
1295 productivity (Bhatia et al., 2013; Gerringa et al., 2012; Hawkins et al., 2014; Herraiz-
1296 Borreguero et al., 2016). The strong melting of the ice shelves can release significant quantities
1297 of freshwater at depth (Biddle et al., 2017), resulting in a strong overturning within the ice
1298 shelves cavity, called the meltwater pump (St-Laurent et al., 2017). Modelling efforts have
1299 identified both resuspended Fe-enriched sediments and CDW entrained to the surface by the
1300 meltwater pump as the two primary sources of dFe to coastal polynyas, providing up to 31% of
1301 the total dFe, compared to 6% for direct ice shelves input (Dinniman et al., 2020; St-Laurent et
1302 al., 2017). Other drivers such as sea-ice coverage (and associated increases in light and dFe
1303 availability when sea ice retreats), or winds have also been shown to impact primary productivity
1304 in polynyas (Park et al., 2019; Park et al., 2017; Vaillancourt et al., 2003).

1306 The key question of how glacial meltwater variability may impact biological productivity in the
1307 ASE has previously been raised during the ASPIRE program (Yager et al., 2012). During the
1308 expedition, a significant supply of melt-laden iron-enriched seawater to the central euphotic zone
1309 of the ASP was observed, potentially explaining why this area is the most biologically
1310 productive in Antarctica (Randall-Goodwin et al., 2015; Sherrell et al., 2015). Other studies in
1311 the Western Antarctic Peninsula and East Antarctica showed that the meltwater pump process
1312 was also responsible for natural Fe supply to the surface, increasing primary productivity (Cape
1313 et al., 2019; Tamura et al., 2022).

1314

1315 In this study, we investigate the long-term relationship between the main environmental factors
1316 of the ASE and the surface biological productivity, with a focus on ice shelves melting. A
1317 demonstrated relationship between glacial meltwater and phytoplankton growth would have far-
1318 reaching consequences for regional productivity in coastal Antarctica, and possibly offshore,
1319 over the coming decades under expected climate change scenarios (Meredith et al., 2019). We
1320 test the hypothesis that changes in glacial meltwater are linked to the surface ocean primary
1321 productivity variability observed over the last two decades. We use a combination of satellite
1322 (ocean color and ice shelf melting rate), climate re-analysis, and model data spanning 1998 to
1323 2017.

1324

1325 2. Material and Methods

1326

1327 2.1 Study area and polynya mapping

1328

1329 We focus on the PIP and ASP in the ASE in West Antarctica (Fig. 1). The ASE is comprised of
1330 several ice shelves and glaciers, including: Abbot (Abb), Cosgrove (Cs), Pine Island (PIG),
1331 Thwaites (Tw), Crosson (Cs), Dotson (Dt) and Getz (Gt). The PIG and Thwaites have received
1332 significant attention in recent years due to their potentially large contribution to sea level rise
1333 (Rignot et al., 2019; Scambos et al., 2017). Along with the Crosson and Dotson ice shelves, the
1334 PIG and Thwaites are undergoing the highest melt rate, which is expected to increase under
1335 climate change scenarios (Naughten et al., 2023; Paolo et al., 2023). The mean mixed-layer
1336 depth (MLD) in the ASP is deeper (Fig. 1b), indicating that it may better entrain deeper sources

Deleted: melt

Deleted: (Meredith et al., 2019).

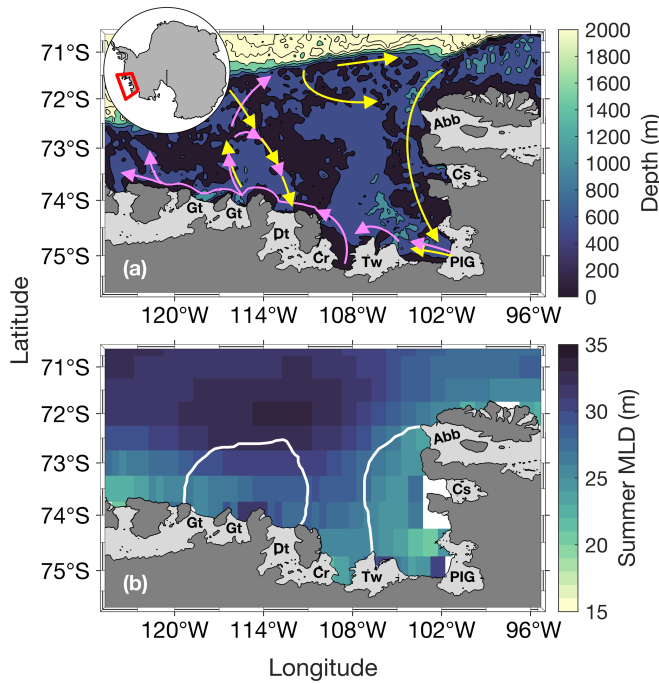
Deleted: melt

Deleted: Materials

Deleted: We focus on the PIP and ASP in West Antarctica (Fig. 1). Polynya boundaries were determined using a 15% sea-ice concentration (SIC) mask (Moreau et al., 2015; Stammerjohn et al., 2008) for every 8-day period from June 1998 to June 2017 to accurately represent the size of the polynya through time.[¶]

Fig. 1. Spatial distribution of (a) annual surface chla during the bloom and (b) net primary productivity (NPP) climatology (1998 – 2017) for the Amundsen (ASP) and Pine Island (PIP) polynyas. The black lines represent the climatological summer polynya boundaries.

1367 of nutrients into the upper waters. The polynyas' boundaries were determined using a 15% sea-
1368 ice concentration (SIC) mask (Moreau et al., 2015; Stammerjohn et al., 2008) for every 8-day
1369 period from June 1998 to June 2017 to accurately represent the size of the polynyas through
1370 time.



1380 **Figure 1.** Study area. Panel 1a shows the bathymetry (from ETOPO1; Amante & Eakins, 2009) ←
1381 and panel 1b shows the climatological summer mixed-layer depth (MLD) from 1998 to 2017.
1382 Panel 1a shows a simplified schematic of the local deep ocean circulation (~ below 400m, yellow
1383 arrows) and upper glacial meltwater/sediments/circumpolar deep water sourced dFe pathways
1384 (magenta arrows), which follows the local upper ocean circulation. Schematic adapted from St-
1385 Laurent et al. (2017). The white lines in panel (b) represent the climatological summer polynyas'
1386 boundaries for the Amundsen Sea polynya (left) and Pine Island polynya (right). The dark grey
1387 area is mainland Antarctica. Light grey areas indicate floating ice shelves and glaciers: Abbot

Formatted: Automatically adjust right indent when grid is defined, Adjust space between Latin and Asian text, Adjust space between Asian text and numbers

Formatted: Font color: Text 1

1398 (Abb), Cosgrove (Cs), Pine Island Glacier (PIG), Thwaites (Tw), Crosson (Cr), Dotson (Dt) and
1399 Getz (Gt).

1400

1401 2.2 Satellite ocean surface chlorophyll-*a* and net primary productivity

1402

1403 We obtained level-3 satellite surface chlorophyll-*a* (chl*a*) concentration with spatial and
1404 temporal resolution of 0.04° and 8 days from the European Space Agency (ESA) Globcolor
1405 project. [We used the CHL1-GSM \(Garver-Siegel-Maritorena\) \(Maritorena and Siegel, 2005\)](https://www.globcolour.info/)
1406 standard Case 1 water merged products consisting of the Sea-viewing Wide Field-of-view
1407 (SeaWiFS), Medium Resolution Imaging Spectrometer (MERIS), Moderate Resolution Imaging
1408 Spectroradiometer (MODIS-A) and Visible Infrared Imaging Suite sensors (VIIRS). [We chose to](#)
1409 [perform our analysis with the merged GlobColour product, which has been widely applied and](#)
1410 [tested in Southern Ocean and coastal Antarctic studies \(Ardyna et al., 2017; Sari El Dine et al.,](#)
1411 [2025; Golder & Antoine, 2025; Nunes, Fereira & Brito, 2025\), to increase our spatial and](#)
1412 [temporal coverage.](#)

1413

1414 [We estimated phytoplankton bloom phenology metrics following the Kauko et al. \(2021\)](#)
1415 [method. Firstly, we applied a spatial 3x3 pixels median filter to reduce gaps in missing data.](#)
1416 [Then, if a pixel was still empty, we applied the average chl*a* of the previous and following week](#)
1417 [to fill the data gap. Data were smoothed using a 4-point moving median \(representing a month of](#)
1418 [data\). For each pixel, the threshold for the bloom detection was based on 1.05 times the annual](#)
1419 [median. The threshold method is frequently used \(Racault et al., 2012; Siegel et al., 2002\) and](#)
1420 [proven reliable at higher latitudes \(Marchese et al., 2017; Soppa et al., 2016; Thomalla et al.,](#)
1421 [2023\). We then determined 5 main bloom metrics. The bloom start \(BS\) is defined as the day](#)
1422 [where chl*a* first exceeds the threshold for at least 2 consecutive 8-day periods. Conversely, the](#)
1423 [bloom end is the day where chl*a* first falls below the threshold for at least 2 consecutive 8-day](#)
1424 [periods. The bloom duration \(BD\) is the time elapsed between bloom start and bloom end. The](#)
1425 [bloom mean chl*a* \(BM\) and bloom max chl*a* are respectively the average and maximum chl*a*](#)
1426 [value calculated during the bloom. Each year is centered around austral summer, from June 10th](#)
1427 [year *n* \(day 1\) to June 9th year *n+1* \(day 365 or 366\). We also averaged our 8-day data to](#)
1428 [monthly data to perform a spatial correlation analysis \(see section 2.6\).](#)

Deleted: (<https://www.globcolour.info/>). We used

Formatted: Not Highlight

Formatted: Font color: Text 1

Deleted: []

[2]

15134

15135 We note that satellite ocean-colour chla algorithms (including the GlobColour merged product
15136 used here) are globally tuned and may underperform in optically complex waters (e.g., with
15137 elevated dissolved organic matter or suspended sediments, ‘Case 2’). In the ASP, past work (e.g.,
15138 Park et al. 2017) shows that satellite chlorophyll climatologies reflect broad seasonal patterns
15139 that are consistent with *in situ* measurements of phytoplankton biomass and photophysiology,
15140 but there is limited data from regions immediately adjacent to glacier fronts or during times of
15141 strong meltwater input. Thus, while we consider satellite chla to be useful for capturing spatial
15142 and temporal variability at polynya scale, uncertainty likely increases in optically complex zones
15143 near glacier margins or during low-light periods, and needs to be considered while interpreting
15144 results.

15145

15146 Eight-day satellite derived Net Primary Productivity (NPP) data with 1/12° spatial resolution,
15147 spanning 1998 - 2017 using the Vertically Generalized Production Model (Behrenfeld and
15148 Falkowski, 1997) were obtained from the Oregon State University website. The VGPM model is
15149 a chlorophyll-based approach and relies on the assumption that NPP is a function of chla,
15150 influenced by light availability and maximum daily net primary production within the euphotic
15151 zone. SeaWiFS-based NPP data span 1998 - 2009, MODIS-based data span 2002 - 2017. To
15152 increase spatial and temporal coverage, we averaged SeaWiFS and MODIS from 2002 to 2009,
15153 where there was valid data for both in a pixel. NPP data were also monthly averaged and used to
15154 compare with chla spatial and temporal patterns.

15155

15156 We caution that our study focuses on surface productivity, and satellites cannot detect under-ice
15157 phytoplankton and sea-ice algal blooms, therefore likely underestimating total primary
15158 productivity (Ardyna et al., 2020; Boles et al., 2020; Douglas et al., 2024; McClish & Bushinsky,
15159 2023; Stoer & Fennel 2024).

15160

15161 2.3 Ice shelves volume flux

15162

15163 We used the latest ice shelf basal melt rate estimates from Paolo et al. (2023). These estimates are
15164 derived from satellite radar altimetry measurements of ice shelves height, and produced on a 3

Deleted: (Behrenfeld & Falkowski, 1997) were obtained from the Oregon State University website.

Formatted: Font color: Blue

Deleted: (Ardyna et al., 2020; Boles et al., 2020).

Deleted: (2023)

15169 km grid every 3 months, with an effective resolution of ~5 km. For this study, our basal melt
15170 record spans June 1998 to June 2017. We calculated ice shelves volume flux rate for every
15171 gridded cell by multiplying the basal melt rate by the cell area. Data were summed for each ice
15172 shelf for a 3-month period. A 5-point (15 months) running mean was applied to reduce noise,
15173 such as spurious effects induced by seasonality on radar measurements over icy surfaces (Paolo
15174 et al., 2016), and data were temporally averaged from October to March to match the SO
15175 phytoplankton growth season (Arrigo et al., 2015), providing yearly mean values. The Abbot,
15176 Cosgrove, Thwaites, Pine Island Glacier, Crosson, Dotson and Getz ice shelves were used to
15177 calculate a single total meltwater volume flux (TVFall) for the ASE to investigate the link with
15178 surface chla and NPP. We also investigated the relationship between each polynyas' productivity
15179 and their closest ice shelf. The Abbot, Cosgrove, PIG and Thwaites ice shelves were used to
15180 calculate the flux rate in the PIP (TVFpip) while the Thwaites, Crosson, Dotson and Getz ice
15181 shelves were chosen for the ASP (TVFasp). The Thwaites was used in both due to its central
15182 position between the two polynyas. [We thereafter use the term glacial meltwater which defines
15183 meltwater resulting from ice shelf melting.](#)

15184 2.4 Simulated dFe distribution

15185 [The spatial distribution of dFe from different sources in the embayment was investigated from
15186 Dinniman et al. \(2020\) model output. The model used is a Regional Ocean Modelling System
15187 \(ROMS\) model, with a 5 km horizontal resolution and 32 terrain following vertical layers and
15188 includes sea-ice dynamics, as well as mechanical and thermodynamic interaction between ice
15189 shelves and the ocean. The model time run spans seven years and simulates fourteen different
15190 tracers to understand dFe supply across the entire Antarctic coastal zone, with the last two years
15191 simulating biological uptake. For the purpose of this study, we only use four different dFe
15192 sources/tracers in the ASE: ice shelf melt, CDW, sediments and sea ice. Each tracer estimation is
15193 independent from each other, meaning that one source does not affect the other, and they have
15194 the same probability for biological uptake by phytoplankton. That is, dFe from all sources can
15195 equally be taken up by phytoplankton. This is parametrized in the model as all iron molecules
15196 being bound to a ligand and therefore remaining in solution in a bioavailable form \(Gledhill &
15197 Buck, 2012\). For a detailed and complete explanation of the model, see Dinniman et al. \(2020\).](#)

Deleted: (Paolo et al., 2016)

Deleted: (Arrigo et al., 2015)

Deleted: (PIG),

Deleted: TVF

Deleted: Spatial distributions of dFe from different sources in the embayment were investigated from Dinniman et al. (2020) model output. The model used is a Regional Ocean Modelling System (ROMS) model, with a 5 km horizontal resolution and 32 terrain following vertical layers and includes sea-ice dynamics, as well as mechanical and thermodynamic interaction between ice shelves and the ocean. The model time run spans seven years and simulates fourteen different tracers to understand dFe supply across the entire Antarctic coastal zone, with the last two years simulating biological uptake. For the purpose of this study, we only use four different dFe sources/tracers in the ASE: ice shelf melt, CDW, sediments and sea ice. Each tracer estimation is independent from each other, meaning that one source does not affect the other, and they have the same probability for biological uptake by phytoplankton. That is, dFe from all sources can equally be taken up by phytoplankton. This is parametrized in the model as all iron molecules being bound to a ligand and therefore remaining in solution in a bioavailable form. For a detailed and complete explanation of the model, see Dinniman et al. (2020).¶

¶ 2.5 Other environmental parameters¶

We used SIC data spanning June 1998 to June 2017 from the National Snow and Ice Data Center (Cavalieri et al., 1996). The data are Nimbus-7 SMMR and SSMI/SSMIS passive microwave daily SIC with 25 km spatial resolution. We computed the sea-ice retreat (IRT) and open water period (OWP) metrics using a 15% threshold (Stammerjohn et al., 2008). Daily data were monthly averaged to perform a spatial correlation analysis (see section 2.6).¶

We collected monthly level-4 Optimum Interpolation Sea Surface Temperature (OISST.v2) 0.25° high resolution dataset from the National Oceanic and Atmospheric Administration (Banzon et al., 2016). Using this dataset compared to others has been proven to be the most suitable for our region of interest (Yu et al., 2023).¶

We obtained monthly Photosynthetically Available Radiation (PAR) from the same Globcolour project at the same spatial and temporal resolution (0.04° and 8 days) as chla.¶

We used monthly averaged ERA5 reanalysis of zonal (u) and meridional (v) surface wind speed at 10 m above the surface (Hersbach et al., 2020).¶

15251 2.5 Other environmental parameters

15252
15253
15254 We used SIC data spanning June 1998 to June 2017 from the National Snow and Ice Data Center
15255 (Cavalieri et al., 1996). The data are Nimbus-7 SMMR and SSMI/SSMIS passive microwave
15256 daily SIC with 25 km spatial resolution. We computed the sea-ice retreat time (IRT) and open
15257 water period (OWP) metrics using a 15% threshold (Stammerjohn et al., 2008). Daily data were
15258 monthly averaged to perform a spatial correlation analysis (see section 2.6).

15259
15260 We collected monthly level-4 Optimum Interpolation Sea Surface Temperature (OISST.v2)
15261 0.25° high resolution dataset from the National Oceanic and Atmospheric Administration
15262 (Huang et al., 2021). Using this dataset compared to others has been proven to be the most
15263 suitable for our region of interest (Yu et al., 2023).

15264
15265 We obtained monthly Photosynthetically Available Radiation (PAR) from the same Globcolour
15266 project at the same spatial and temporal resolution (0.04° and 8 days) as chla.

15267
15268 We used monthly averaged ERA5 reanalysis of zonal (u) and meridional (v) surface wind speed
15269 at 10 m above the surface (Hersbach et al., 2020).

15270
15271 We finally investigated monthly mean MLD from the Estimating the Circulation and Climate of
15272 the Ocean (ECCO) ocean and sea-ice state estimate project (ECCO consortium et al., 2021). The
15273 dataset is the version 4, release 4, at 0.5° spatial resolution.

15274 2.6 Statistical analysis

15275
15276 Because some of our data were not normally distributed, we consistently applied nonparametric
15277 tests throughout our statistical analysis. A Mann-Kendall test was performed to detect linear
15278 trends in chla and NPP. A two-tailed non-parametric Spearman correlation metric (*rho*, *p*) was
15279 calculated to investigate the relationship between chla, NPP, and glacial meltwater, as well as
15280 between phytoplankton and sea-ice phenology metrics. A two-tailed Mann-Whitney test was

15282 performed to detect any significant mean differences for chla, sea-ice phenology metrics, MLD,
15283 PAR and dFe sources between the two polynyas. Monthly spatial correlations were tested
15284 between SIC, winds, chla, NPP, SST, and PAR after removing the seasonality for each
15285 parameter. As well, a yearly spatial correlation between chla, NPP and TVFall was performed.
15286 The relationships between chla concentration, NPP and environmental factors were explored
15287 using a Principal Component Analysis (PCA). No pre-treatment (mean-centering or
15288 normalization) was applied to the variables prior to PCA, as all variables are expressed in
15289 comparable units and ranges, consistent with common practice in marine biogeochemistry
15290 studies (Marchese et al., 2017; Liniger et al., 2020). Every statistical test was run with a 95% (p-
15291 value < 0.05) confidence level. Our study spans 1998-2017. We are constrained by the start of
15292 satellite ocean color data (1998) and the end of the ice shelf basal melt rate record (2017) from
15293 Paolo et al (2023).

Deleted: and

Formatted: Font: Italic

Deleted: A monthly

Deleted: correlation was

Deleted: TVF

Deleted: (2023)

15295 3. Results

15296

15297 3.1 Glacial meltwater and chla variability

Deleted: melt

15298 The annual climatology maps reveal substantially higher chla concentration and NPP in the ASP
15299 compared to the PIP (Fig. 2). The chla concentration starts increasing in mid-November to reach
15300 its average earlier in the PIP than the ASP. At its peak, chla in the ASP is 6.49 mg m^{-3} and 4.94 mg m^{-3} in the PIP (Fig. 3a). During the bloom period, chla concentration is also higher in the
15301 ASP on average compared to the PIP ($\text{ASP} = 5.21 \pm 1.29 \text{ mg m}^{-3}$; $\text{PIP} = 3.69 \pm 1.11 \text{ mg m}^{-3}$,
15302 Fig. 3b; Supplementary Table T1; p-value < 0.01). When looking at polynya area integrated
15303 values (concentration multiplied by area gives units of mg m^{-1}), chla is significantly higher in the
15304 ASP than in the PIP, and increases with the polynya area (Supplementary Figs. S1 and S2). NPP
15305 is also significantly higher in the ASP than in the PIP ($1.88 \pm 1.12 \text{ TgC y}^{-1}$ vs $0.85 \pm 0.86 \text{ TgC y}^{-1}$,
15306 p-value = 0.004, Supplementary Fig. S3). No significant interannual trends in mean chla and
15307 NPP during the bloom are observed for either polynya (Fig. 3b; Supplementary Fig. S3; p-
15308 value > 0.1).
15309
15310
15311

Moved down [1]: During the bloom period, chla concentration is also higher in the ASP on average compared to the PIP ($\text{ASP} = 5.21 \pm 1.29 \text{ mg m}^{-3}$; $\text{PIP} = 3.69 \pm 1.11 \text{ mg m}^{-3}$, Fig. 2b)

Deleted: 1

Deleted: 2b and Table T1, p-value < 0.01).

Moved (insertion) [1]

Deleted: 2a).

Deleted:,

Deleted: 2b,

Deleted:,

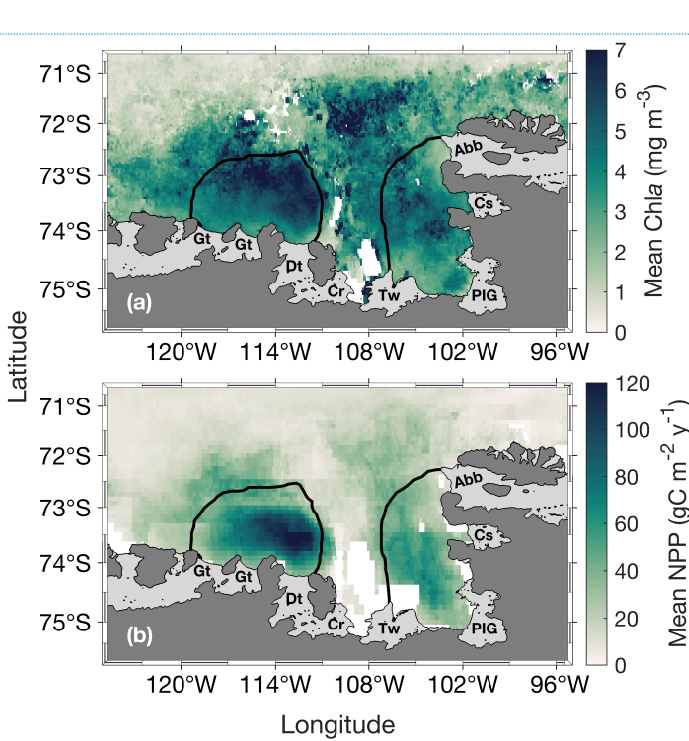


Fig. 2. [Spatial distribution of \(a\) surface chlorophyll-a \(chl a\) during the bloom and \(b\) net primary productivity \(NPP\) climatology \(1998 – 2017\) for the Amundsen \(ASP\) and Pine Island \(PIG\) polynyas. The black lines represent the climatological summer polynyas' boundaries.](#)

Deleted: <object>

Formatted: Automatically adjust right indent when grid is defined, Adjust space between Latin and Asian text, Adjust space between Asian text and numbers

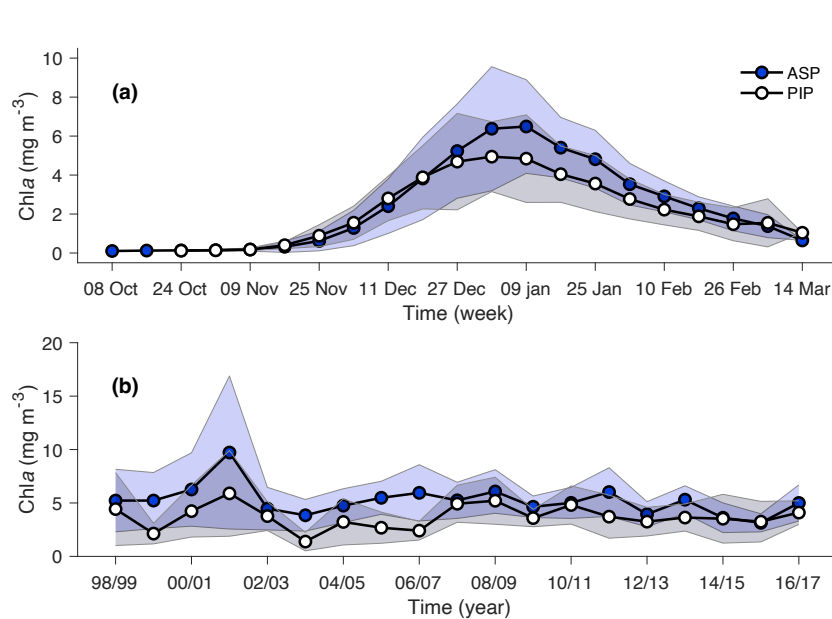


Fig. 3. (a) Weekly chlorophyll-*a* (chl_{*a*}) climatology (1998-2017) for ASP (blue circles) and PIP (white circles). (b) Bloom mean chl_{*a*} time series of ASP (blue circles) and PIP (white circles). Shaded areas represent the standard deviation for a given year. The relationship between chl_{*a*} (in mg m⁻³ and mg m⁻¹) and the polynya size is shown in [Supplementary Fig. S2](#).

The variability in [TVFall](#) is statistically uncorrelated with surface chl_{*a*} concentration and NPP in both polynyas from 1998 to 2017 (Fig. 4; [Supplementary Fig. S4](#)). However, the relationship becomes strongly significant in the ASP for both mean and max chl_{*a*} when we remove the chl_{*a*} outlier in 2001/02 (red data point, Figs. 4a-b), although not for NPP ([Supplementary Figs. S4a-b](#)). The positive relationship implies that surface chl_{*a*} in the ASP is higher when more glacial meltwater is delivered to the embayment. No strong relationships are observed in the PIP between [TVFall](#), surface chl_{*a*} and NPP (Figs. 4c-d; [Supplementary Figs. S4c-d](#)). When fluxes from individual glaciers are considered, PIP chl_{*a*} does not correlate with Abbot, Cosgrove, PIG, Thwaites or TVFpip fluxes (Table 1). On the other hand, ASP chl_{*a*} shows strong relationships with TVFasp, the Dotson [and Crosson](#) ice [shelves](#) (Table 1), and all ice shelves become

Deleted: filled

Formatted: Font: Bold

Deleted: open

Deleted: filled

Deleted: open

Deleted: TVF

Deleted: 3;

Formatted: Font: Italic

Deleted: ,

Deleted: 3a

Deleted: TVF

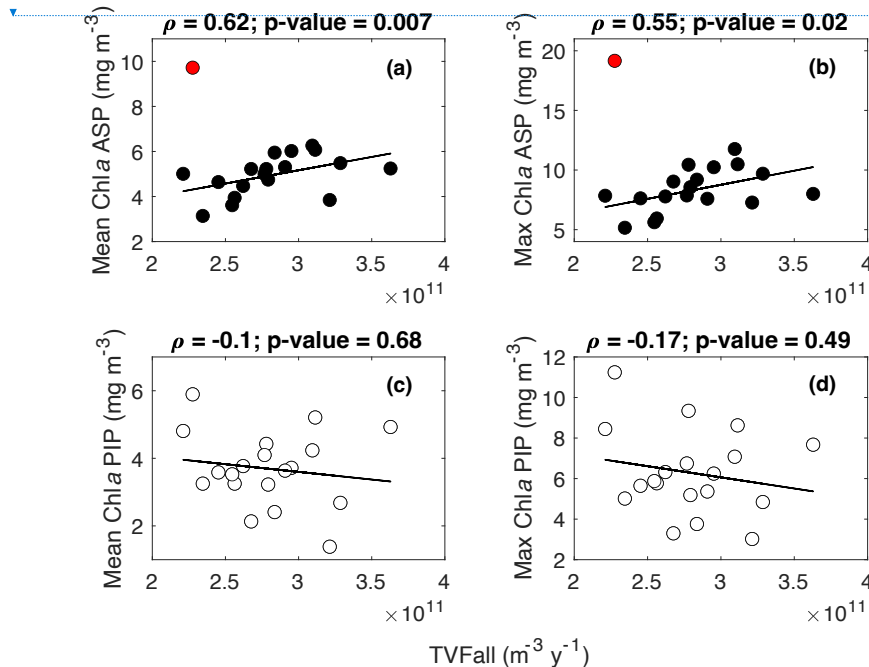
Deleted: 3c

Deleted: and

Deleted: shelf

Deleted:). Note that

15404 significantly correlated with mean and max chla when year 2001/02 is removed. There are no
 15405 statistically significant relationships between individual ice shelves and NPP in both polynyas.
 15406 Spatially, the mean and max chla are strongly correlated with TVFall in southern-eastern part of
 15407 the ASP, in front of the Dotson ice shelf (Figs. 5a-b), where a positive relationship with NPP is
 15408 also observed (Fig. 5c), although not significant.



15428 **Fig. 4.** Scatter plots of mean and max surface chlorophyll-*a* (chla) with the total volume flux
 15429 (TVFall) for (a-b) the ASP and (c-d) the PIP from 1998 to 2017 (n=19). The fitted lines and
 15430 statistics exclude year 2001/02 (red outlier) for the ASP regressions. If all data is considered, the
 15431 relationships between mean chla, max chla and TVFall in the ASP are not significant. TVFall is
 15432 an annual integral representing the sum of all ice shelves (see methods section) for the ASE.

15434 **Table 1.** Statistical summary of the relationships between ice shelves volume flux and

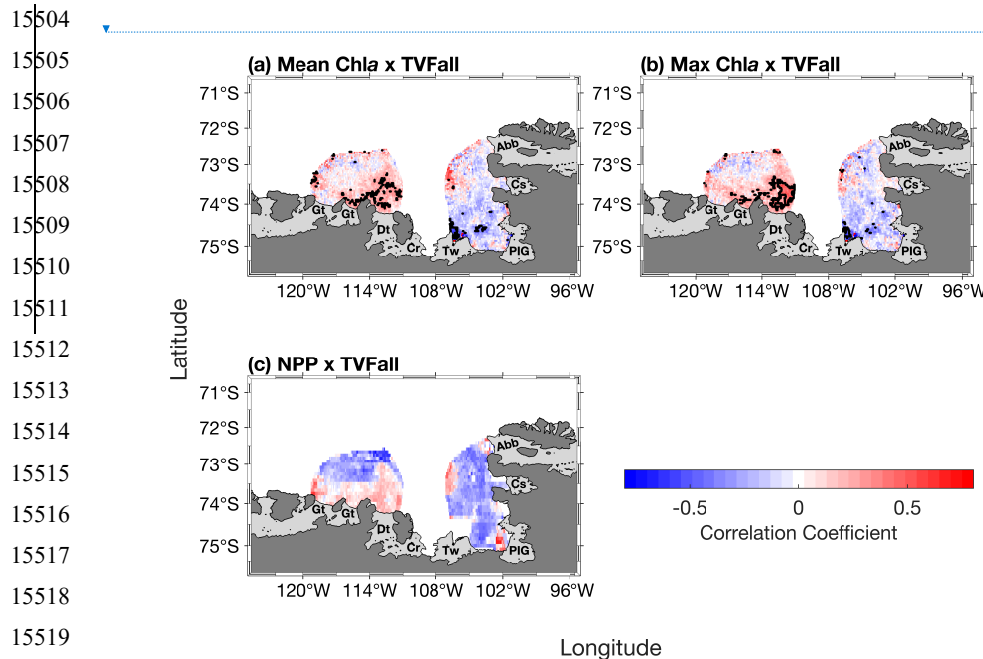
Deleted: the
Deleted: year
Deleted: Note that all ice shelves become significantly correlated with mean and max chla when the 2001/02 year is removed. ...
Deleted: were
Deleted: On the other hand, ASP chla shows strong relationships TVFasp (Table 1).
Deleted: TVF
Deleted: the central
Deleted: 4a
Deleted:
Deleted: 4c
Deleted: <object>

Deleted: 3
Deleted: TVF
Deleted: .
Deleted: the
Deleted: year
Deleted: TVF
Deleted: asp
Deleted: TVF
Deleted:
Deleted: metrics

15459 surface chlorophyll-*a* (chl_a). The * marks a significant (p-value < 0.05) relationship. [Statistical](#)
 15460 [results for the ASP include all years \(n=19\)](#). All relationships between mean chl_a, max chl_a and
 15461 [ASP ice shelves become significant when year 2001/02 is removed](#).

	ASP				PIP			
	Mean chl _a		Max chl _a		Mean chl _a		Max chl _a	
	rho	p-value	rho	p-value	rho	p-value	rho	p-value
Abbot	/	/	/	/	0.09	0.73	-0.04	0.88
Cosgrove	/	/	/	/	-0.32	0.18	-0.46	0.05
PIG	/	/	/	/	-0.04	0.88	-0.13	0.61
Thwaites	0.16	0.52	0.11	0.66	0.12	0.63	0.09	0.71
Crosson	0.43	0.07	0.50	0.03*	/	/	/	/
Dotson	0.48	0.04*	0.54	0.02*	/	/	/	/
Getz	0.37	0.12	0.43	0.07	/	/	/	/
TVFasp	0.42	0.07	0.46	0.05*	/	/	/	/
TVFpip	/	/	/	/	0.009	0.97	-0.1	0.68

Formatted	[6]
Formatted	[7]
Formatted	[3]
Formatted	[4]
Formatted Table	[5]
Formatted	[10]
Formatted	[11]
Formatted	[12]
Formatted	[13]
Formatted	[8]
Formatted	[9]
Formatted	[16]
Formatted	[18]
Formatted	[19]
Formatted	[20]
Formatted	[22]
Formatted	[14]
Formatted	[17]
Formatted	[21]
Formatted	[23]
Formatted	[15]
Formatted	[24]
Formatted	[25]
Formatted	[26]
Formatted	[27]
Formatted	[28]
Formatted	[29]
Formatted	[30]
Formatted	[31]
Formatted	[32]
Formatted	[33]
Formatted	[34]
Formatted	[35]
Formatted	[36]
Formatted	[37]
Formatted	[38]
Formatted	[39]
Formatted	[40]
Formatted	[41]
Formatted	[42]
Formatted	[43]
Formatted	[44]
Formatted	[45]
Formatted	[46]
Formatted	[47]
Formatted	[48]
Formatted	[49]
Formatted	[50]
Formatted	[51]
Formatted	[52]
Formatted	[53]
Formatted	[55]
Formatted	[56]



Deleted: 1

... [114]

Fig. 5. Spatial correlation maps between total volume flux (TVFall) and (a) surface mean chlorophyll-a (chl), (b) surface max chl and (c) net primary productivity (NPP) (n=19). The black contour represents significant correlations at 95% confidence level. Data outside of the summer climatological polynyas boundaries were masked out.

Deleted: 4

Deleted: TVF

Deleted: crosses represent

Deleted: correlation

Deleted: polynyas

3.2 Simulated dFe sources distribution

The modelled spatial distribution of surface dFe sources is presented in Fig. 6. On average, the smallest dFe source in the embayment is from the ice shelves, with a maximum concentration between the Thwaites and Dotson ice shelves. The dFe from sea ice is slightly higher than from ice shelves and similar over the two polynyas, and is higher near the sea-ice margin (Fig. 6b). The dFe from CDW is also higher between the Thwaites and Dotson (Fig. 6c). Sediment is the dominant dFe source (Fig. 6d). Its distribution spreads from 108°W to the western part of the Getz ice shelf. The highest sediment concentration is found along the coast and inside the ASP. On

Deleted: distributions

Deleted: are

Deleted: 5

Deleted: (

Deleted: 5a),

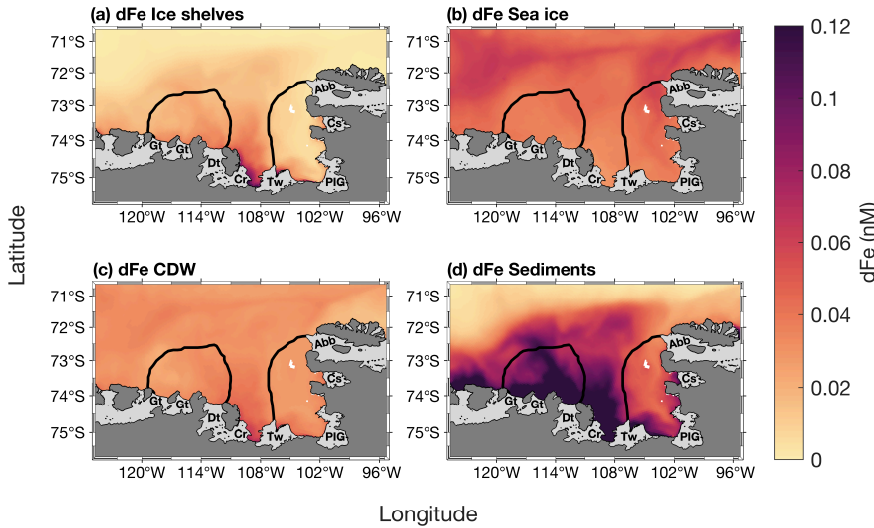
Formatted: Font: Bold

Deleted: 5b

Deleted: 5c

Deleted: 5d

15550 polynya-wide average basis, the sediment reservoir contributes significantly more to total dFe in
 15551 the ASP (58.3%, 0.13nM) compared to sea ice (16.5%, 0.04nM), CDW (13.5%, 0.03nM) and ice
 15552 shelves (11.7%, 0.03nM). In the PIP, the contribution of sediments is still significantly higher
 15553 (41.2%; 0.08nM) but lower than the ASP and the contribution gap with the other sources decreases.
 15554 The CDW and sea ice contribute 22.5% (0.04nM) and 18.9% (0.035nM) to the dFe pool
 15555 respectively, while ice shelves are still the smallest sources at 14.5% (0.03nM) in the PIP.



15556
 15557 **Fig. 6.** Two-years top-100m averaged spatial distribution of surface dissolved iron (dFe)
 15558 contribution from (a) ice shelves, (b) sea ice, (c) circumpolar deep water (CDW) and (d) sediments
 15559 simulated by the model from Dinniman et al. (2020). The black lines represent the climatological
 15560 polynyas' boundaries.
 15561

15562 3.3 Environmental parameters, chla and NPP variability

15563 During the phytoplankton growth season (October-March), SIC is spatially significantly
 15564 anticorrelated to the meridional winds speed in both polynyas (Fig. 7a). Chla is significantly
 15565 positively correlated with SST in the eastern ASP, and the whole PIP (Fig. 7b), but weakly with

Deleted:

[115]

Deleted: **Fig. 5.** Two-years top-100m averaged spatial distribution of surface dissolved iron (dFe) contribution from (a) ice shelves, (b) sea ice, (c) circumpolar deep water and (d) sediments simulated by the model from Dinniman et al. (2020). The black lines represent the climatological summer polynya boundaries.

Deleted: 6a

Deleted: central-

Deleted: 6b

15593 PAR in both polynyas (Fig. 7c). Finally, PAR and SST are positively [related](#) in both central
 15594 polynyas, albeit not significantly (Fig. 7d). We note that similar spatial relationships are
 15595 observed when NPP is correlated with SST and PAR. ([Supplementary](#) Fig. S5).

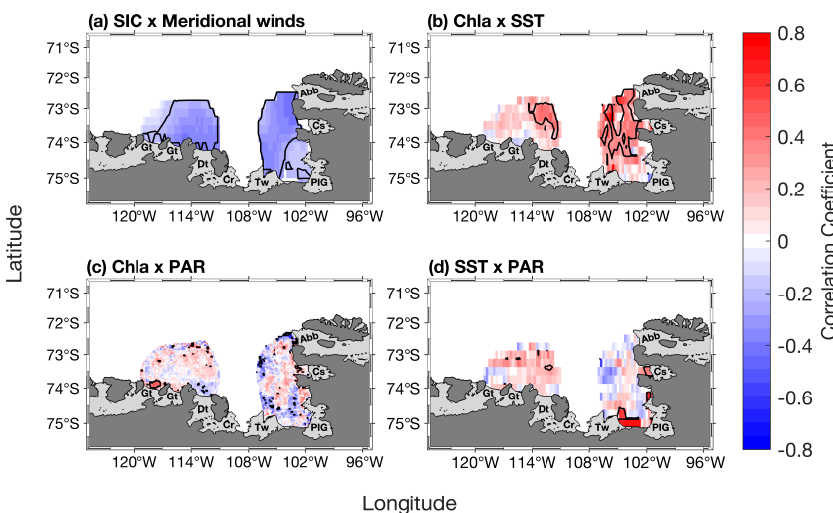
Deleted: 6c

Deleted: linked

Deleted: 6d

Deleted: 

... [116]



15611 **Fig. 7.** Spatial correlation [map](#) between sea-ice concentration (SIC) and (a) meridional winds.
 15612 Spatial correlation maps between [mean](#) chlorophyll-*a* (chla) concentration and (b) sea surface
 15613 temperature (SST), (c) photosynthetically available radiation (PAR). (d) Spatial correlation [map](#)
 15614 between PAR and SST. Data span 1998 – 2017 from October to March (n=114). The black [contour](#)
 15615 [represents](#) significant [correlations](#) at 95% confidence level. Seasonality was removed from the data
 15616 before [performing](#) the correlation. Data outside of the summer climatological [polynyas](#)
 15617 boundaries were masked out.

Deleted: 6

Deleted: maps

Deleted: (mg m⁻³)

Deleted: crosses represent

Deleted: correlation

Deleted: preforming

Deleted: polynyas

15618 Regarding the phenology, the bloom start is positively correlated to IRT and negatively with
 15619 OWP in the ASP, although not significantly with the OWP (Table 2). This means that the bloom
 15620 starts earlier and later as IRT does, and that longer OWP and earlier bloom starts are correlated
 15621 with earlier ice retreat. The bloom mean and bloom max chla are not correlated with either IRT
 15622 and OWP in the ASP. [IRT and OWP are significantly related \(p = -0.93; p-value < 0.001\). When](#)

Formatted: Normal (Web)

15639 year 2001/02 is removed, no significant changes in the relationships between all parameters are
 15640 detected. In the PIP, all metrics are significantly related to each other, except for PAR and OWP
 15641 (Table 2). That is, the bloom start is positively correlated with IRT and negatively with OWP,
 15642 while the bloom duration, mean chla, max chla concentrations and NPP are negatively linked to
 15643 the IRT and positively with OWP. SST and PAR are negatively correlated with IRT, and
 15644 positively with SST. IRT and OWP are significantly related in the PIP, (p = -0.88; p-value <
 15645 0.001).

Deleted: to
Deleted: while OWP is only significantly
Deleted: correlated to
Deleted: .

15646
 15647 **Table 2.** Statistical summary of the relationships between the phytoplankton bloom metrics and
 15648 environmental parameters (n=19). The * marks a significant (p-value < 0.05) relationship. IRT =
 15649 ice retreat time, OWP = open water period, NPP = net primary productivity, SST = sea surface
 15650 temperature, PAR = photosynthetically available radiation. Removing year 2001/02 for the ASP
 15651 slightly changes the strength of the relationships between parameters (i.e., rho) but not the
 15652 significance.

Deleted: and sea-ice phenology
Deleted: .

	Amundsen Sea polynya				Pine Island polynya				
	IRT		OWP		IRT		OWP		
		rho	p-value	rho	p-value	rho	p-value	rho	p-value
Bloom start	0.51	0.03*	-0.43	0.07	0.56	0.02*	-0.48	0.04*	
Bloom duration	-0.12	0.63	0.09	0.71	-	0.02*	0.59	0.01*	
Bloom mean	0.19	0.44	-0.33	0.17	-	0.003*	0.50	0.04*	
Bloom max	0.24	0.32	-0.35	0.14	-	0.005*	0.52	0.03*	
NPP	-0.55	0.02*	0.45	0.05	-	0.001*	0.54	0.02*	

Deleted: 04
Deleted: 08
Deleted: 60
Deleted: 72
Deleted: 20
Deleted: 35
Deleted: 16
Deleted: 25
Deleted: 36
Deleted: 52

15670	SST	-0.09	0.72	-0.01	0.96	-	0.02*	0.52	0.03*
15671	PAR	-0.09	0.72	0.05	0.84	-	0.007*	0.38	0.12

15672

15673

15674

15675

15676

15677

15678

15679

15680

15681

15682

15683

15684

15685 We explore the relationships between phytoplankton bloom [phenology metrics](#) and their
 15686 potential environmental drivers by conducting a multivariate PCA for both polynyas (Fig. 8).
 15687 [The PCA reduces our datasets \(11 variables\) and breaks them down into dimensions that capture](#)
 15688 [most of the variability and relationships between all variables. Arrows indicate the contribution](#)
 15689 [of each variable to the dimensions, with longer arrows representing stronger influence.](#)
 15690 [Observations \(in our case, years\) positioned in the direction of an arrow are more influenced by](#)
 15691 [that variable.](#) In the ASP (Fig. 8a), the first two principal components explain 55.3% of the total
 15692 variance (Dim1: 35%, Dim2: 20.3%). NPP in the ASP is closely associated with BD, indicating
 15693 that [the bloom duration is the primary driver](#) of production. On the other hand, environmental
 15694 vectors such as TVFall and TVFasp [project](#) more strongly onto Dim2 with the bloom mean chla,
 15695 indicating that meltwater input may influence surface chla interannual variability, and is less
 15696 directly tied to NPP. We note that when [year](#) 2001/02 is removed, the relationship between
 15697 TVFasp and TVFall becomes much stronger with the bloom mean chla ([Supplementary](#) Fig.
 15698 [S6a](#)) and is slightly [anticorrelated](#) to SST and MLD. In the PIP (Fig. 8b), the first two
 15699 components [account](#) for 63.7% of the total variance (Dim1: 46.7%, Dim2: 17%). Compared to
 15700 the ASP, both NPP and BM [cluster](#) strongly with BD and PAR [on Dim1](#). Additionally, [IRT](#),

Deleted: 07

Deleted: 79

Deleted: 03

Deleted: 91

Deleted: 11

Deleted: 66

Deleted: 09

Deleted: 71

Deleted: 13

Deleted: phenologies

Formatted: Normal (Web), Space After: 12 pt

Deleted: 7).

Deleted: 7a

Deleted: 58.1

Formatted: Font color: Text 1

Deleted: 37.9

Deleted: 2

Deleted: PAR and

Deleted: light availability and

Deleted: are

Deleted: drivers

Deleted: projected

Deleted: the

Deleted: summer

Deleted: S7a

Deleted: anti correlated

Deleted: 7b

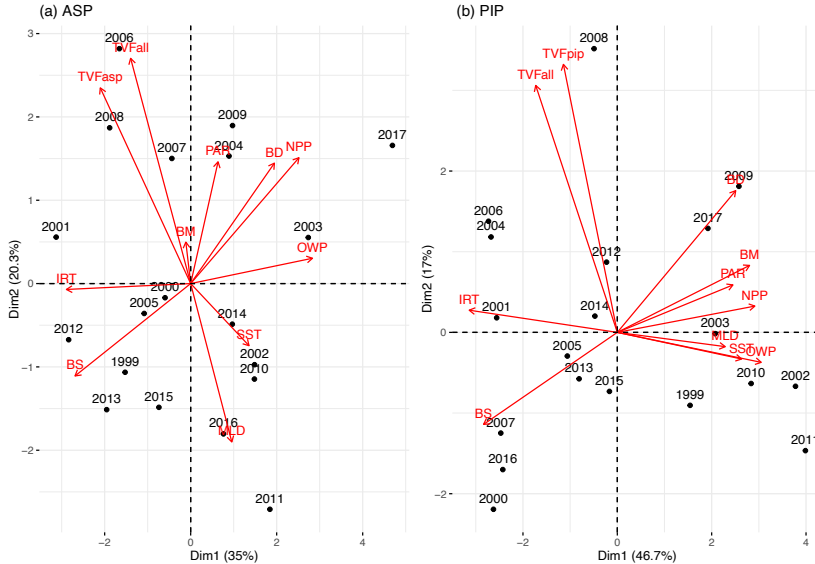
Deleted: accounted

Deleted: 66.9

Deleted: 48.2

Deleted: 18.7

Deleted: clustered



15731 OWP and SST and MLD aligned along Dim1, which explains 46.7% of the total variance
 15732 compared to 35% for the ASP, suggesting that physical conditions might play a stronger
 15733 structuring role in PIP compared to the ASP. In contrast, TVFall and TVFpip stand alone and
 15734 align more strongly with Dim2, suggesting a less dominant influence of meltwater on the system
 15735 bloom mean chla and NPP variability in the PIP. Finally, polynya-averaged PAR and MLD are
 15736 significantly stronger and deeper, respectively, in the ASP compared to the PIP during the bloom
 15737 season (MLD ASP = 28.5 ± 5.7 m; MLD PIP = 24.9 ± 3.7 m; p-value = 0.03 and PAR ASP = 31.5 ± 5.4 Einstein $m^{-2} d^{-1}$; PAR PIP = 26.5 ± 6.7 Einstein $m^{-2} d^{-1}$; p-value = 0.02).

Formatted: Font color: Auto

15739
 15740
 15741
 15742
 15743
 15744
 15745
 15746

Deleted: <object>

15749

15750

15751

15752

15753

15754

15755

15756

15757 **Fig. 8.** Principal component analysis biplot of environmental parameters (red) and years (black) for (a) the ASP and (b) the PIP. TVFasp = total volume flux for ASP; TVFpip = total volume flux for PIP; TVFall = total volume flux for all ice shelves; BM = bloom mean; PAR = photosynthetically available radiation; BD = bloom duration; NPP = net primary productivity; OWP = open water period; SST = sea surface temperature; MLD = mixed-layer depth; BS = bloom start; IRT = ice retreat time. The same plot is presented in supplementary Fig. S6, but removing year 2001/02 for the ASP, emphasizing the relationship between total volume flux (TVFall, TVFasp) and BM in the ASP.

15765

15766 4. Discussion

15767

15768 4.1 Effect of glacial meltwater on phytoplankton chla and NPP

15769

15770 The relationship between glacial meltwater, surface chla and NPP observed over the last two
15771 decades was distinctly different between the two polynyas. In the ASP, we found that enhanced
15772 glacial melt translates into higher surface chla, but not with NPP (when removing year 2001/02;
15773 Figs. 4a-b; Supplementary Fig. S6a). Modelling results (Fig. 6) suggest that sediment from the
15774 seafloor is the main source of dFe in the ASP, but this source is also linked to glacial melt. Ice
15775 shelf glacial meltwater drives the meltwater pump, which brings up mCDW and fine-grained
15776 subglacial sediments to the surface. This result is in agreement with previous research: Melt-
15777 laden modified CDW flowing offshore from the Dotson ice shelf to the central ASP (Sherrell et
15778 al., 2015), and resuspended sediments (Dinniman et al., 2020; St-Laurent et al., 2017; 2019) have
15779 been identified as significant sources of dFe to be used by phytoplankton. Interestingly, both dFe

Formatted: Font color: Black

Deleted: 7

Deleted: Same

Deleted: Figure S7

Deleted: the

Deleted: anomalous year

Deleted: fluxes

Deleted: the bloom mean (

Deleted:)

Formatted: Font: Not Bold, English (US)

Deleted: ice shelf

Deleted: The relationship between glacial melt rates and surface chla observed over the last two decades was distinctly different between the two polynyas. In the ASP, we found that enhanced glacial melt translates into higher surface chla, but not with NPP (when removing the anomalous 2001/02 summer; Figs. 3a-b; Fig. S7a). Modelling results (Fig. 5) suggest that sediment from the seafloor is the main source of dFe in the ASP, but this source is also linked to glacial melt. Ice shelf glacial meltwater drives the meltwater pump, which brings up modified CDW (mCDW) and fine-grained subglacial sediments to the surface. This result is in agreement with previous research: Melt-laden modified CDW flowing offshore from the Dotson ice shelf to the central ASP (Sherrell et al., 2015), and resuspended sediments (Dinniman et al., 2020; St-Laurent et al., 2017; 2019) have been identified as significant sources of dFe to be used by phytoplankton. Interestingly, both dFe supplied from ice shelves and CDW are most important in front of the Thwaites and Crosson ice shelves, where the area averaged basal melt rate, and thus likely the area averaged meltwater pumping (Jourdain et al., 2017) are typically strongest in observations (Adusumilli et al., 2020; Rignot et al., 2013) and the modelling (Fig. 5). The year 2001/02 does not stand out as being influenced by any specific parameter in the ASP compared to other years (Fig. 7a; Fig. S7a). The anomalously high surface chla observed during this year, as also reported by Arrigo et al. (2012), may result from exceptional conditions that were not captured by the parameters analysed in our study - for instance, an imbalance in the grazing pressure. Interestingly, surface chla and NPP exhibit contrasting trends when averaged across the polynya. While TVF may explain some of the variance in surface chla, it does not account for the variance in NPP, whether assessed through direct or multivariate relationships. This decoupling between chla and NPP in the ASP suggests that ice shelf meltwaters, while enhancing surface phytoplankton biomass through nutrient delivery, also promote vertical mixing. This mixing deepens the mixed layer, reducing light availability and constraining photosynthetic rates. These rates are influenced by fluctuations in the MLD, even in the presence of high biomass and sufficient macronutrients. Additionally, interannual variability in the composition of the phytoplankton community may further explain these observations. For example, the occasional dominance of the small prymnesiophyte *Phaeocystis antarctica*, a low- [117]

15883 supplied from ice shelves and CDW are most important in front of the Thwaites and Crosson ice
15884 shelves, where the area averaged basal melt rate, and thus likely the area averaged meltwater
15885 pumping (Jourdain et al., 2017), are typically strongest in observations (Adusumilli et al., 2020;
15886 Rignot et al., 2013) and the modelling (Fig. 6). The year 2001/02 does not stand out as being
15887 influenced by any specific parameter in the ASP compared to other years (Fig. 8a,
15888 Supplementary Fig. S6a). The anomalously high surface chla observed during this year, as also
15889 reported by Arrigo et al. (2012), may result from exceptional conditions that were not captured
15890 by the parameters analysed in our study, for instance, an imbalance in the grazing pressure.
15891 Interestingly, surface chla and NPP exhibit contrasting trends when averaged across the polynya.
15892 While TVFall may explain some of the variance in surface chla, it does not account for the
15893 variance in NPP, whether assessed through direct or multivariate relationships. This decoupling
15894 between chla and NPP in the ASP suggests that glacial meltwater, while enhancing surface
15895 phytoplankton biomass through nutrient delivery, may also promote vertical mixing. This mixing
15896 deepens the mixed layer, reducing light availability and constraining photosynthetic rates. These
15897 rates are influenced by fluctuations in the MLD, even in the presence of high biomass and
15898 sufficient macronutrients. The summer MLD is deeper in the ASP (Fig. 1b), which would
15899 decrease light availability, despite higher PAR compared to the PIP. Previous studies report that
15900 the small prymnesiophyte *P. antarctica*, a low-efficiency primary producer (Lee et al., 2017), is
15901 better adapted to deeper mixed layers and therefore lower light conditions (Alderkamp et al.,
15902 2012; Mills et al., 2010) and could contribute to high surface chla decoupled from NPP, as
15903 observed in the ASP. This is consistent with past *in situ* studies showing systematic differences
15904 in mixed-layer structure between the two polynyas. The PIP commonly exhibits a shallow,
15905 strongly stratified surface mixed layer while the ASP is more variable and has been observed to
15906 host deeper MLD (Alderkamp et al., 2012; Park et al., 2017; Yager et al., 2016; Mills et al.,
15907 2012).
15908
15909 In the PIP, we did not find any long-term relationships between the phytoplankton bloom, NPP
15910 and glacial meltwater. Variability in ice shelf glacial meltwater may not have the same effect on
15911 the surface chla and NPP in the PIP compared to the ASP. Iron delivered from glacial melt
15912 process related in the PIP and west of it could accumulate and follow the westward coastal
15913 current, towards the ASP (St-Laurent et al., 2017). These sources would include dFe from

Deleted: relationship

Deleted: melt rates

Deleted: (St-Laurent et al., 2017)

15917 meltwater pumped CDW, sediments and ice shelves, all of which are higher in front of the
15918 Crosson ice shelf, west of the PIP (Fig. 6). With the coastal circulation, this would make dFe
15919 supplied by glacial meltwater greater in the ASP, thereby contributing to the higher productivity
15920 in the ASP. Recently, subglacial discharge (SGD) was shown to have a different impact on basal
15921 melt rate in the ASE polynyas (Goldberg et al., 2023), where PIG had a lot less relative increase
15922 in melt with SGD input than Thwaites or Dotson/Crosson. Thus, assuming a direct relationship
15923 between meltrate, SGD and dFe sources, the signal in the PIP (fed by PIG melt) will be much
15924 weaker than in the ASP (fed by upstream Thwaites, Crosson and local Dotson due to the
15925 circulation), which might also explain the discrepancies between the PIP and ASP. [A stronger](#)
15926 [meltwater-driven stratification may also dominate in the PIP, reducing vertical nutrient](#)
15927 [replenishment and thereby limiting biomass growth \(Oh et al., 2022\), even where TVFall is high,](#)
15928 [hence leading to a direct negative relationship observed compared to the ASP \(Fig. 4;](#)
15929 [Supplementary Fig. S4\).](#) The model outputs used here are critical to understand the spatial
15930 distribution of dFe in the embayment. They strongly suggest, but do not definitively demonstrate,
15931 the role of dFe in influencing the phytoplankton bloom interannual variability.

Deleted: 5

15932
15933 [The decoupling between surface chla and NPP could reflect two contrasting meltwater effects.](#)
15934 [Near glacier and ice-shelf fronts, entrainment of iron-rich deep waters rising to the surface](#)
15935 [through the meltwater pump can produce surface chla maxima \(high biomass\) without](#)
15936 [proportional increases in depth-integrated productivity. Further from the coast, meltwater](#)
15937 [spreading at neutral buoyancy strengthens stratification, limiting vertical nutrient fluxes and](#)
15938 [thereby suppressing NPP despite elevated chla. These dual mechanisms are consistent with](#)
15939 [observational and modelling studies of meltwater entrainment and dispersal \(Randall-Goodwin et](#)
15940 [al., 2015; St-Laurent et al., 2017; Dinniman et al., 2020; Forsch et al. 2021\), and suggest that](#)
15941 [spatial heterogeneity in plume dynamics could explain the observed chla and NPP mismatch. We](#)
15942 [also note as a limitation that satellite-derived chla and VGPM NPP estimates lack the vertical](#)
15943 [resolution needed to resolve sub-plume stratification and mixing processes \(e.g., fine-scale](#)
15944 [vertical gradients in iron or nutrient fluxes\), so our mechanistic interpretations of surface chla vs.](#)
15945 [depth-integrated productivity decoupling must be taken with caution.](#)

Formatted: Font color: Black

Deleted: 5

... [118]

16104 Satellite algorithms commonly estimate NPP from surface chla, but the approach and
16105 assumptions vary across models. The VGPM relates chla to depth-integrated photosynthesis
16106 through empirical relationships with light and temperature (Behrenfeld & Falkowski, 1997). In
16107 contrast, the Carbon-based Productivity Model (CbPM) emphasizes phytoplankton carbon
16108 biomass and growth rates derived from satellite optical properties, decoupling productivity
16109 estimates from chla alone (Westberry et al., 2008). The CAFE model (Carbon, Absorption, and
16110 Fluorescence Euphotic-resolving model) integrates additional physiological parameters such as
16111 chla fluorescence and absorption to better constrain phytoplankton carbon fixation (Silsbe et al.,
16112 2016). In the Southern Ocean, where light limitation, iron supply, and community composition
16113 strongly influence the relationship between chla and productivity, these algorithmic differences
16114 can yield substantial variability in NPP estimates (Ryan-Keogh et al., 2023), with studies
16115 showing that VGPM-type models often outperform CbPM in coastal Southern Ocean regions
16116 (Jena et al., 2020). Because the VGPM algorithm does not explicitly incorporate the MLD, but
16117 instead estimates primary production integrated over the euphotic zone based on surface chla,
16118 PAR, and temperature, it may not fully capture the influence of variable MLD or subsurface
16119 processes related to glacial melt, which could contribute to the observed decoupling between
16120 chla and NPP. Therefore, while the observed decoupling between chla and NPP in the ASP
16121 might also come from our choice of dataset, the VGPM model may be more appropriate for
16122 coastal polynya environments, such as those in the Amundsen Sea.

16123

16124 Direct observations from Sherrell et al. (2015) showed higher chla in the central ASP while
16125 surface dFe was low weeks before the bloom peak. This suggests a continuous supply and
16126 consumption of dFe in the area, most likely from the circulation, as mentioned above.
16127 Considering the long residence time of water masses in both polynyas (about 2 years (Tamsitt et
16128 al., 2021)), and the daily dFe uptake by phytoplankton (3-196 pmol l⁻¹ d⁻¹ (Lannuzel et al.,
16129 2023)), we also hypothesise that any dFe reaching the upper ocean from external sources is
16130 quickly used and unlikely to remain readily available for phytoplankton in the following spring
16131 season.

16132

16133 In recent model simulations with the meltwater pump turned off, Fe becomes the principal factor
16134 limiting phytoplankton growth in the ASP (Oliver et al., 2019). However, the transport of Fe-rich

16135 [glacial meltwater outside the ice shelf cavities and to the ocean surface depends strongly on the](#)
16136 [local hydrography. While Naveira Garabato et al. \(2017\) suggested that the glacial meltwater](#)
16137 [concentration and settling depth \(neutral buoyancy\) outside the ice shelf cavities is controlled by](#)
16138 [an overturning circulation driven by instability, others suggest that the strong stratification plays](#)
16139 [an important role in how close to the surface the buoyant plume of said meltwater can rise](#)
16140 [\(Arnscheidt et al., 2021; Zheng et al., 2021\). Therefore, high melting years and greater TVFall](#)
16141 [might not necessarily translate into a more iron-enriched meltwater delivered to the surface](#)
16142 [outside the ice shelf cavities, close to the ice shelf edge, as rising water masses may be either](#)
16143 [prevented from doing so, or be transported further offshore in the polynyas where the](#)
16144 [phytoplankton bloom occurs, before they can resurface \(Herraiz-Borreguero et al., 2016\).](#)

16145

16146 [Although several Fe sources can fuel polynya blooms, and they depend on processes mentioned](#)
16147 [above, Fe-binding ligands may ultimately set the limit on how much of this dFe stays dissolved](#)
16148 [in the surface waters \(Gledhill and Buck, 2012; Hassler et al., 2019; Tagliabue et al., 2019\).](#)

16149 [Models of the Amundsen Sea \(Dinniman et al., 2020, 2023; St-Laurent et al., 2017, 2019\) did not](#)
16150 [include Fe complexation with ligands and assumed a continuous supply of available dFe for](#)
16151 [phytoplankton. Spatial and seasonal data on Fe-binding ligands along the Antarctic coast remain](#)
16152 [extremely scarce and their dynamics are poorly understood \(see Smith et al. \(2022\) for a](#)
16153 [database of publicly available Fe-binding ligand surveys performed south of 50°S\). Field](#)
16154 [observations in the ASP and PIP suggest that the ligands measured in the upwelling region in](#)
16155 [front of the ice shelves had little capacity to complex any additional Fe supplied from glacial](#)
16156 [melt. As a consequence, much of the glacial and sedimentary Fe supply in front of the ice](#)
16157 [shelves could be lost via particle scavenging and precipitation \(Thuróczy et al., 2012\). This was](#)
16158 [also recently observed by van Manen et al. \(2022\) in the ASP. However, within the polynya](#)
16159 [blooms, Thuróczy et al. \(2012\) found that the ligands produced by biological activity were](#)
16160 [capable of stabilising additional Fe supplied from glacial melt, where we observed the highest](#)
16161 [productivity. The production of ligands by phytoplankton would increase the stock of](#)
16162 [bioavailable dFe and further fuel the phytoplankton bloom in the polynyas, potentially](#)
16163 [highlighting the dominance of *P. antarctica*, which uses iron-binding ligands more efficiently](#)
16164 [than diatoms \(Thuróczy et al., 2012\), even under low light conditions. Model development and](#)
16165 [sustained field observations on dFe availability, including ligands, are needed to adequately](#)

16166 predict how these may impact biological productivity under changing glacial and oceanic
16167 conditions, now and in the future.

16168
16169 Overall, the discrepancies observed between the ASP and PIP point to a complex set of ice-
16170 ocean-sediment interactions, where several co-occurring processes and differences in
16171 hydrographic properties of the water column influence dFe supply and consequent primary
16172 productivity.

16173
16174 4.2 Possible drivers of the difference in phytoplankton surface chla and NPP between the
16175 two polynyas

16176
16177 The biological productivity is higher in the ASP than the PIP, consistent with previous studies
16178 (Arrigo et al., 2012; Park et al., 2017). In section 4.1, we mentioned the underlying hydrographic
16179 drivers of these differences. We related the higher biological productivity in the ASP to a
16180 potentially greater supply of iron from melt-laden Fe-enriched mCDW and sediment sources, but
16181 this difference in productivity could also be attributed to other local features. The Bear Ridge
16182 grounded icebergs on the ASP's eastern side (Bett et al., 2020) could add to the overall
16183 meltwater pump strength. They can enhance warm CDW intrusions to the ice shelf cavity (Bett
16184 et al., 2020), increasing ice shelf melting and subsequent stronger phytoplankton bloom from the
16185 meltwater pump activity. These processes are weaker or absent in the PIP. Few sources other
16186 than glacial meltwater may influence the bloom in the PIP. For instance, dFe in the euphotic
16187 zone can also be sustained by the biological recycling, as shown in the PIP by Gerringa et al.
16188 (2020).

16189
16190 Sea ice could also partly explain the difference in chla magnitudes, NPP, and variability between
16191 the ASP and PIP. The strong spatial correlation between SIC and meridional winds (Fig. 7a)
16192 indicates that southerly winds can export the coastal sea ice offshore and play a significant role
16193 in opening the polynyas. In the ASP compared to the PIP, sea ice retreats earlier (IRT = Jan 1st ±
16194 14d vs Jan 18th ± 17d, p-value = 0.003), the open water period is longer (OWP = 61 ± 16d vs 44
16195 ± 22d, p-value < 0.001), and the SIC is lower (Supplementary Fig. S7). In the ASP, an early sea-
16196 ice retreat leads to an earlier bloom start, but the longer open water period is not significantly

Formatted: Normal (Web)

Deleted: S6c, Table 2

16198 associated with greater bloom mean and max chla (Table 2). On the other hand in the PIP, an
16199 early sea-ice retreat also triggers an early bloom start, but the longer open duration is associated
16200 with warmer water, higher bloom mean chla, max chla, and NPP. These results suggest that
16201 different processes might drive phytoplankton growth variability in the two polynyas. In the
16202 ASP, it is likely the replenishment of dFe mentioned above that mostly influences the bloom. In
16203 the PIP, higher SIC can delay the retreat time and shorten the open water season (Table 2, [Supplementary Fig. S7](#)), leading to lower chla and NPP compared to the ASP. The significant
16204 negative relationships between IRT, PAR, chla and NPP in the PIP (Table 2, [Supplementary Fig. S6](#)) suggests a strong light limitation relief in the polynya. This light limitation hypothesis is
16205 further supported by the high correlation between polynya-averaged chla mean with PAR and
16206 SST in the PIP across the 19 years of study, compared to the lack of correlation in the ASP ([Supplementary Table T2](#); p-value < 0.01 for all relationships in the PIP). While *P. antarctica* is
16207 usually the main phytoplankton species dominating in both polynyas, the combination of light-
16208 limitation relief and higher SST may create better conditions for a stratified and warmer
16209 environment that would favor diatom (Arrigo et al., 1999; van Leeuwe et al., 2020), as recently
16210 observed in the ASP (Lee et al., 2022). The positive association of PAR, SST and chla with
16211 MLD likely reflects conditions around sea-ice retreat (all negatively associated with IRT), when
16212 enhanced wind mixing deepens the mixed layer and replenishes surface nutrients while light
16213 availability and SST increases. This nutrient-light co-limitation phase supports high biomass
16214 accumulation, likely from diatoms. Similar results have been reported by [Park et al. \(2017\)](#). They
16215 found that the PIP was dFe replete, potentially from biological recycling ([Gerringa et al., 2020](#)),
16216 compared to an iron-limited ASP. We hypothesise that the connection between glacial meltwater
16217 and chla that we found in the ASP is a response to iron input (also observed by [Park et al. \(2017\)](#)
16218 during incubation experiments) compared to the PIP, where light and temperature seem to play a
16219 more significant role in driving the phytoplankton bloom variability. Our results suggest
16220 potential long-term changes in the phytoplankton community, specifically a shift towards
16221 diatoms in the ASE coastal regions during phytoplankton bloom. Hayward et al. (2025) reported
16222 a decline in diatoms from 1997 to 2017 in the PIP. However, they observed an increase in
16223 diatoms after 2017, linked to regime shift in sea ice. Their study also indicates that diatoms are
16224 competitively disadvantaged under iron-depleted conditions. *P. antarctica*, which relies on dFe
16225 supplied by ocean circulation, would then tends to dominate in the ASP. Such shifts in

Deleted: the

Deleted: ;

Deleted: S6

Deleted: less light availability and

Deleted: phytoplankton productivity

Deleted: relationship

Deleted: ;

Deleted: compared to the lack of correlation in the ASP (Table T2; p-value < 0.01 for all relationships in the PIP).

Deleted: Park et al. (2017)

Formatted: Font color: Black

Deleted: ([Gerringa et al., 2020](#))

Deleted: ice shelf

Deleted: Park et al. (2017)

16242 phytoplankton composition are likely to affect carbon export, grazing, and higher trophic levels.
16243 Additional long-term data on inter-annual variability in phytoplankton composition and
16244 physiology will be essential to fully understand these relationships.

Formatted: Font color: Auto

16245
16246 Variability in SIC and sea-ice retreat can be influenced by the Amundsen Sea Low (ASL). We
16247 therefore also investigated its potential role on sea-ice variability. We found on average weak
16248 spatial negative relationships between SIC and ASL latitude, longitude, mean sector and actual
16249 central pressure in both polynyas during the growing seasons (Supplementary Fig. S8), and only
16250 slightly significant in the eastern PIP. The weak relationships might be owing to the seasonal
16251 variation of the ASL, where its position largely varies during summer, and its impact in shaping
16252 coastal sea ice is also greater during winter and autumn in the Amundsen-Bellingshausen region
16253 (Hosking et al., 2013). The lack of strong significant relationships overall does not allow us to
16254 conclude that the ASL plays an important role in shaping the coastal polynyas landscape and
16255 influencing chla variability.

16256 4.3 Limitations and future directions

16257
16258 While it seems reasonable that the higher ASP productivity could be driven by more iron
16259 delivered through a stronger meltwater pump downstream of the PIP, our data cannot confirm
16260 this hypothesis. To accurately understand the role of iron through the meltwater pump process,
16261 we would need to quantify the fraction of meltwater and glacial modified water (mix of CDW
16262 and ice shelf meltwater) reaching the ocean surface, together with the iron content. Obtaining
16263 this information is challenging over the decadal time scales considered and the method used in
16264 our study. Here, our intention was to provide valuable insights into the potential drivers of our
16265 results, and highlight the benefit of remote sensing, in this poorly observed environment. Our
16266 work directly aligns with Pan et al. (2025), who investigated the long-term relationship between
16267 sea surface glacial meltwater and satellite surface chla in the Western Antarctic Peninsula, and
16268 found a strong relationship between the two parameters, highlighting the importance of glacial
16269 meltwater discharge in regions prone to extreme and rapid climate changes.

16270
16271
Deleted: Variability in SIC and sea-ice retreat can be influenced by the Amundsen Sea Low (ASL; Hosking et al., 2013; Turner et al., 2016). We therefore also investigated its potential role on sea-ice variability. We found on average weak spatial negative relationships between SIC and ASL latitude, longitude, mean sector and actual central pressure in both polynyas during the growing seasons (Fig. S8), and only slightly significant in the eastern PIP. The weak relationships might be owing to the seasonal variation of the ASL, where its position largely varies during summer, and its impact in shaping coastal sea ice is also greater during winter and autumn in the Amundsen-Bellingshausen region (Hosking et al., 2013). The lack of strong significant relationships overall does not allow us to conclude that the ASL plays an important role in shaping the coastal polynyas landscape and influencing chla variability.¶

¶ 4.3 Limitations and future directions¶

¶ While it seems reasonable that the higher ASP productivity could be driven by more iron delivered through a stronger meltwater pump downstream of the PIP, our data cannot confirm this hypothesis. To accurately understand the role of iron through the meltwater pump process, we would need to quantify the fraction of meltwater and glacial modified water (mix of CDW and ice shelf meltwater) reaching the ocean surface, together with the iron content. Obtaining this information is challenging over the decadal time scales considered and the method used in our study. Here, our intention was to provide insights into the potential drivers of our results, and highlight the benefit of remote sensing

16303 In multimodel climate change simulations, Naughten et al (2018) showed an increase of ice
16304 shelves melting up to 90% on average, attributed to more warm CDW on the shelf, due to
16305 atmospherically driven changes in local sea-ice formation. More recently, Dinniman et al. (2023)
16306 also highlighted the impact of projected atmospheric changes on Antarctic ice sheet melt. They
16307 showed that strengthening winds, increasing precipitation and warmer atmospheric temperatures
16308 will increase heat advection onto the continental shelf, ultimately increasing basal melt rate by
16309 83% by 2100. Compared to present climate simulations, their simulation showed a 62% increase
16310 in total dFe supply to shelf surface waters, while basal melt driven overturning Fe supply
16311 increased by 48%. The ice shelf melt and overturning contributions varied spatially, increasing in
16312 the Amundsen-Bellingshausen area and decreasing in East Antarctica. This implies that, under
16313 future climate change, phytoplankton productivity could show stronger spatial asymmetry
16314 around Antarctica. The increasing melting and thinning of ice shelves will eventually result in
16315 more numerous calving events and drifting icebergs (Liu et al., 2015). Model simulations
16316 stressed the importance of ice shelves and icebergs in delivering dFe to the SO (Death et al.,
16317 2014; Person et al., 2019), increasing offshore productivity. As Fe will likely be replenished and
16318 sufficient from increasing melting in coastal areas, it is possible that the system will shift from
16319 Fe-limited to being limited by nitrate, silicate, or even manganese (Anugerahan & Tagliabue,
16320 2024), while offshore SO productivity will likely remain Fe-dependent (Oh et al., 2022).

16322 5. Conclusions

16323 Using spatial and multivariate approaches, our study explored the variability of surface chla and
16324 NPP in the Amundsen Sea polynyas over the last two decades, with a focus on the main
16325 environmental characteristics of the ASE. We found a potential strong relationship between ice
16326 shelf melting and surface chla in the ASP, which becomes stronger when year 2001/02 was
16327 removed, a result in agreement with the ASPIRE field studies and previous satellite analyses. On
16328 the other hand, we did not find clear evidence of such a relationship in the PIP, where light, sea
16329 surface temperature and open water availability seem more important. The differences between
16330 the polynyas may lie in hydrographic properties, or the use of satellite remote sensing itself,
16331 which cannot tell us about processes such as Fe supply, bioavailability and phytoplankton
16332 demand. To gain greater insight, we referred to model simulations that showed the spatial

Deleted: In multimodel climate change simulations, Naughten et al (2018) showed an increase of ice shelves melting up to 90% on average, attributed to more warm CDW on the shelf, due to atmospherically driven changes in local sea-ice formation. More recently, Dinniman et al. (2023) also highlighted the impact of projected atmospheric changes on Antarctic ice sheet melt. They showed that strengthening winds, increasing precipitation and warmer atmospheric temperatures will increase heat advection onto the continental shelf, ultimately increasing basal melt rate by 83% by 2100. Compared to present climate simulations, their simulation showed a 62% increase in total dFe supply to shelf surface waters, while basal melt driven overturning Fe supply increased by 48%. The ice shelf melt and overturning contributions varied spatially, increasing in the Amundsen-Bellingshausen area and decreasing in East Antarctica. This implies that, under future climate change, phytoplankton productivity could show stronger spatial asymmetry around Antarctica. The increasing melting and thinning of ice shelves will eventually result in more numerous calving events and drifting icebergs (Liu et al., 2015). Model simulations stressed the importance of ice shelves and icebergs in delivering dFe to the SO (Death et al., 2014; Person et al., 2019), increasing offshore productivity. As Fe will likely be replenished and sufficient from increasing melting in coastal areas, it is possible that the system will shift from Fe-limited to being limited by nitrate, silicate, or even manganese (Anugerahan & Tagliabue, 2024), while offshore SO productivity will likely remain Fe-dependent (Oh et al., 2022).¶

¶ 5. Conclusions¶

Using spatial and multivariate approaches, our study explored the variability of surface chla and NPP in the Amundsen Sea polynyas over the last two decades, with a focus on the main environmental characteristics of the ASE.

Deleted: the anomalous

Deleted: summer

16373 variability in the magnitude of iron sources. Our results call for sustained *in situ* observations
16374 (e.g., moorings equipped with trace-metal clean samplers, and physical sensors to better
16375 understand year-to-year water mass meltwater fraction and properties) to elucidate these long-
16376 term relationships. Satellite observations are a powerful tool to investigate the relationship
16377 between glacial meltwater and biological productivity on such time scales, which has until now
16378 relied almost exclusively on field observations and modelling. Using such tools, we showed how
16379 the relationship between phytoplankton and the environment varies spatially and temporally
16380 across 19 years.

16381 Appendices

16382 No appendices are related to the manuscript.

16383

16384 Data availability

16385 Bathymetry data (Amante & Eakins, 2009) was taken from the NOAA website
16386 (<http://www.ngdc.noaa.gov/mgg/global/global.html>). Mixed-layer depth (ECCO Consortium et
16387 al., 2021) can be accessed here:
16388 https://podaac.jpl.nasa.gov/dataset/ECCO_L4_MIXED_LAYER_DEPTH_05DEG_MONTHLY_V4R4. Satellite surface chlorophyll-*a* and photosynthetically available radiation were
16389 downloaded from <https://www.globcolour.info/>. Sea surface temperature (Huang et al., 2021)
16390 can be found here <https://psl.noaa.gov/data/gridded/data.noaa.oisst.v2.highres.html>. Wind re-
16391 analysis data (Hersbach et al., 2020) are available at
16392 <https://cds.climate.copernicus.eu/datasets/reanalysis-era5-single-levels-monthly-means?tab=download>. Sea-ice concentration (Cavalieri et al., 1996) was obtained from
16393 <https://nsidc.org/data> and Net Primary productivity (Behrenfeld and Falkowski, 1997) was
16394 downloaded from <http://sites.science.oregonstate.edu/ocean/productivity/index.php>. Circumpolar
16395 surface model output from Dinniman et al (2020) can be found at <https://www.bco-dmo.org/dataset/782848>. The Amundsen Sea Low index (Hosking et al., 2016) data are available
16396 at http://scotthosking.com/asl_index.

16401 Author contributions

16402

Deleted: .

Deleted: ice

Deleted: Satellite surface chlorophyll-*a* and photosynthetically available radiation were downloaded from <https://www.globcolour.info/>. Sea surface temperature (Banzon et al., 2016) can be found here <https://psl.noaa.gov/data/gridded/data.noaa.oisst.v2.highres.html>. Wind re-analysis data (Hersbach et al., 2020) are available at <https://cds.climate.copernicus.eu/cdsapp#!/dataset/10.24381/cds.f17050d7?tab=form>. Sea-ice concentration (Cavalieri et al., 1996) was obtained from <https://nsidc.org/data> and Net Primary productivity (Behrenfeld & Falkowski, 1997) was downloaded from <http://sites.science.oregonstate.edu/ocean/productivity/index.php>. Circumpolar surface model output from Dinniman et al (2020) can be found at <https://www.bco-dmo.org/dataset/782848>. The Amundsen Sea Low index (Hosking et al., 2016) data are available at http://scotthosking.com/asl_index.

Author contributions

GL conceptualised and led the study; MSD provided the dissolved iron model output. All authors were involved in the interpretation of the results, the revision, and the writing of the final version of the paper.

Competing interest

We declare having no competing interests.

Acknowledgments

We would like to thank the University of Tasmania, the Australian Research Council (ARC) Centre of Excellence for Climate Extremes (CE170100023), and the Australian Centre for Excellence in Antarctic Science (ACEAS; SR200100008) for financial support. Delphine Lannuzel is funded by the ARC through a Future Fellowship (L0026677). Sébastien Moreau received funding from the Research Council of Norway (RCN) for the project “I-CRYME: Impact of CRYosphere Melting on Southern Ocean Ecosystems and biogeochemical cycles” (grant number 335512) and for the Norwegian Centre of Excellence “iC3: Center for ice, Cryosphere, Carbon and Climate” (grant number 332635). Michael Dinniman was supported by the U.S National Science Foundation grant OPP-1643652. We are also grateful to Will Hobbs, Rob Massom and Patricia Yager for their knowledgeable input. We thank Vincent Georges for some preliminary work as part of his masters’ internship. We are very grateful to Fernando S. Paolo for his early input and help with the ice shelf meltwater dataset.

16453 GL conceptualised and led the study; MSD provided the dissolved iron model output. All authors
16454 were involved in the interpretation of the results, the revision, and the writing of the final version
16455 of the paper.

16456

16457 **Competing interest**

16458 We declare having no competing interests.

16459

16460 **Acknowledgments**

16461 We would like to thank the University of Tasmania, the Australian Research Council (ARC)
16462 Centre of Excellence for Climate Extremes (CE170100023), and the Australian Centre for
16463 Excellence in Antarctic Science (ACEAS; SR200100008) for financial support. Delphine
16464 Lannuzel is funded by the ARC through a Future Fellowship (L0026677). Sebastien Moreau
16465 received funding from the Research Council of Norway (RCN) for the project “I-CRYME:
16466 Impact of CRYosphere Melting on Southern Ocean Ecosystems and biogeochemical cycles”
16467 (grant number 335512) and for the Norwegian Centre of Excellence “iC3: Center for ice,
16468 Cryosphere, Carbon and Climate” (grand number 332635). Michael Dinniman was supported by
16469 the U.S National Science Foundation grant OPP-1643652. We are also grateful to Will Hobbs,
16470 Rob Massom and Patricia Yager for their knowledgeable input. We thank Vincent Georges for
16471 some preliminary work as part of his masters’ internship. We are very grateful to Fernando S.
16472 Paolo for his early input and help with the glacial meltwater dataset. We thank the data providers
16473 mentioned in the methods section for making their data available and free of charge.

16474

16475 **Financial support**

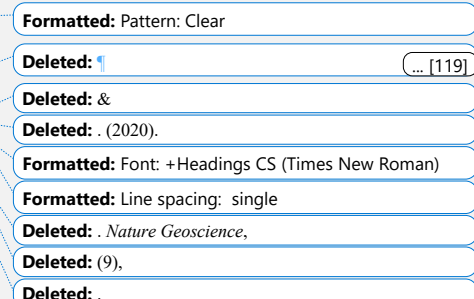
16476 All financial support were mentioned in the Acknowledgment section.

16477

16478 **References**

16479 Adusumilli, S., Fricker, H. A., Medley, B., Padman, L., and Siegfried, M. R.: Interannual
16480 variations in meltwater input to the Southern Ocean from Antarctic ice shelves, *Nat. Geosci.*, 13,
16481 616–620, <https://doi.org/10.1038/s41561-020-0616-z>, 2020.

16482 Alderkamp, A-C., Mills, M. M., van Dijken, G. L., Lann, P., Thuróczy, C-E., Gerringa, L. J.A.,
16483 de Barr, H. J. W., Payne, C. D., Visser, R. J. W., Buma A. G. J., and Arrigo, K. R.: Iron from
16484 glaciers fuels phytoplankton blooms in the Amundsen Sea (Southern Ocean): Phytoplankton



16492 characteristics and productivity. *Deep-Sea Res. II.*, 71–76, 32–48,
 16493 <https://doi.org/10.1016/j.dsr2.2012.03.005>, 2012.

16494

16495 Amante, C., and Eakins, B.W.:ETOPO1 1 Arc-Minute Global Relief Model: Procedures, Data
 16496 Sources and Analysis, NOAA Technical Memorandum NESDIS NGDC-24. National
 16497 Geophysical Data Center [data set], NOAA, doi:10.7289/V5C8276M, 2009.

16498

16499 Anugerahananti, P., and Tagliabue, A.: Response of Southern Ocean Resource Stress in a Changing Climate. *Geophys. Res. Lett.*, 51, e2023GL107870, <https://doi.org/10.1029/2023GL107870>, 2024.

16500

16501

16502 Ardyna, M., Claustre, H., Sallée, J.-B., D'Ovidio, F., Gentili, B., van Dijken, G. L., D'Ortenzio, F., and Arrigo, K. R.: Delineating environmental control of phytoplankton biomass and phenology in the Southern Ocean, *Geophys. Res. Lett.*, 44, 5016–5024, doi:10.1002/2016GL072428, 2017.

16503

16504

16505

16506 Ardyna, M., Mundy, C. J., Mayot, N., Matthes, L. C., Oziel, L., Horvat, C., Leu, E., Assmy, P., Hill, V., Matrai, P. A., Gale, M., Melnikov, I. A., and Arrigo, K. R.: Under-Ice Phytoplankton Blooms: Shedding Light on the “Invisible” Part of Arctic Primary Production. *Front. Mar. Sci.*, 7, <https://doi.org/10.3389/fmars.2020.608032>, 2020.

16507

16508

16509

16510 Arnscheidt, C. W., Marshall, J., Dutrieux, P., Rye, C. D., and Ramadhan, A.: On the Settling Depth of Meltwater Escaping from beneath Antarctic Ice Shelves. *JPO*, 51, 2257–2270, <https://doi.org/10.1175/JPO-D-20-0286.1>, 2021.

16511

16512

16513 Arrigo, K. R., Lowry, K. E., and van Dijken, G. L.: Annual changes in sea ice and phytoplankton in polynyas of the Amundsen Sea, Antarctica. *Deep-Sea Res. II.*, 71–76, 5–15, <https://doi.org/10.1016/j.dsr2.2012.03.006>, 2012.

16514

16515

16516 Arrigo, K. R., Robinson, D. H., Worthen, D. L., Dunbar, R. B., DiTullio, G. R., VanWoert, M., and Lizotte, M. P.: Phytoplankton community structure and the drawdown of nutrients and CO₂ in the Southern Ocean, *Sci.*, 283, 5400, 365–367, DOI: 10.1126/science.283.5400.365, 1999.

16517

16518

16519

16520 Arrigo, K. R. and van Dijken, G. L.: Phytoplankton dynamics within 37 Antarctic coastal polynya systems. *J. Geophys. Res. Ocean.*, 108, <https://doi.org/10.1029/2002JC001739>, 2003.

16521

16522 Arrigo, K. R., van Dijken, G. L., and Strong, A. L.: Environmental controls of marine productivity hot spots around Antarctica. *J. Geophys. Res. Ocean.*, 120, 5545–5565, <https://doi.org/10.1002/2015JC010888>, 2015.

16523

16524

16525 Arrigo, K. R., Worthen, D., Schnell, A., and Lizotte, M. P.: Primary production in Southern Ocean waters. *J. Geophys. Res. Ocean.*, 103, 15587–15600, <https://doi.org/10.1029/98JC00930>, 1998.

16526

16527

16528 Assmann, K. M., Jenkins, A., Shoosmith, D. R., Walker, D., Jacobs, S., and Nicholls, K.: Variability of circumpolar deep water transport onto the Amundsen Sea continental shelf through

16529

Deleted: .., &
Deleted: . (2024).
Formatted: Line spacing: single
Deleted: . *Geophysical Research Letters*,
Deleted: (10),
Deleted: .
Deleted: et al. (2020).
Formatted: Line spacing: single
Deleted: . *Frontiers in Marine Science*,
Deleted: .
Deleted: &
Deleted: . (2021).
Deleted: *Journal of Physical Oceanography*
Deleted: (7),
Deleted: .
Deleted: &
Deleted: . (2012).
Deleted: .
Deleted: Research Part
Deleted: : *Topical Studies in Oceanography*,
Deleted: Arrigo, K. R., & van Dijken, G. L. (2003).
Formatted: Line spacing: single
Deleted: . *Journal of Geophysical Research: Oceans*,
Deleted: (C8).
Deleted: &
Deleted: . (2015).
Deleted: *Journal of Geophysical Research: Oceans*,
Deleted: (8),
Deleted: .
Deleted: &
Deleted: . (1998).
Deleted: . *Journal of Geophysical Research: Oceans*,
Deleted: (C8),
Deleted: .
Deleted: Banzon, V., Smith, T. M., Chin, T. M., Liu, C., & Hankins, W. (2016). A long-term record of blended satellite and in situ sea-surface temperature for climate monitoring, modeling and environmental studies. *Earth System Science Data*, 8(1), 165–176. <https://doi.org/10.5194/essd-8-165-2016>

16566 a shelf break trough. *J. Geophys. Res. Oceans*, 118, 6603–6620, doi:10.1002/2013JC008871, 16567 2013.

16568 Behrenfeld, M. J. *and* Falkowski, P. G.: Photosynthetic rates derived from satellite-based 16569 chlorophyll concentration. *Limnol. Oceanogr.*, 42, 1–20, 16570 https://doi.org/10.4319/lo.1997.42.1.0001, 1997.

Deleted: .., &... and Falkowski, P. G. (1997)....: Photosynthetic rates derived from satellite-based chlorophyll concentration. *Limnology and Oceanography*,..., *Limnol. Oceanogr.*, 42(1),..., 1–20. (... [120])

16571 Bett, D. T., Holland, P. R., Naveira Garabato, A. C., Jenkins, A., Dutrieux, P., Kimura, S., *and* 16572 Fleming, A.: The Impact of the Amundsen Sea Freshwater Balance on Ocean Melting of the 16573 West Antarctic Ice Sheet. *J. Geophys. Res. Oceans*, 125, https://doi.org/10.1029/2020JC016305, 16574 2020.

Formatted: Line spacing: single

Deleted: . N..., Jenkins, A., Dutrieux, P., Kimura, S., &...nd Fleming, A. (2020)....: The Impact of the Amundsen Sea Freshwater Balance on Ocean Melting of the West Antarctic Ice Sheet. *Journal of Geophysical Research:... J. Geophys. Res. Oceans*,..., 125(9). (... [121])

16575 Bhatia, M. P., Kujawinski, E. B., Das, S. B., Breier, C. F., Henderson, P. B., *and* Charette, M. A.: 16576 Greenland meltwater as a significant and potentially bioavailable source of iron to the ocean. 16577 *Nat. Geosci.*, 6, 274–278, https://doi.org/10.1038/ngeo1746, 2013.

Deleted: ..&nd Charette, M. A. (2013)....: Greenland meltwater as a significant and potentially bioavailable source of iron to the ocean. *Nature Geoscience*... *Nat. Geosci.*, 6(4),..., 274–278.... (... [122])

16578 Biddle, L. C., Heywood, K. J., Kaiser, J., *and* Jenkins, A.: Glacial Meltwater Identification in the 16579 Amundsen Sea. *JPO*, 47, 933–954, https://doi.org/10.1175/JPO-D-16-0221.1, 2017.

Deleted: &...nd Jenkins, A. (2017)....: Glacial Meltwater Identification in the Amundsen Sea. *Journal of Physical Oceanography*... *JPO*, 47(4),..., 933–954. (... [123])

16580 Boles, E., Provost, C., Garçon, V., Bertosio, C., Athanase, M., Koenig, Z., *and* Sennéchal, N.: 16581 Under-Ice Phytoplankton Blooms in the Central Arctic Ocean: Insights From the First 16582 Biogeochemical IAOOS Platform Drift in 2017. *J. Geophys. Res. Ocean.*, 125, e2019JC015608, 16583 https://doi.org/10.1029/2019JC015608, 2020.

Deleted: &...nd Sennéchal, N. (2020)....: Under-Ice Phytoplankton Blooms in the Central Arctic Ocean: Insights From the First Biogeochemical IAOOS Platform Drift in 2017. *Journal of Geophysical Research: Oceans*,..., *J. Geophys. Res. Ocean.*, 125(3),..., e2019JC015608. (... [124])

16584 Boyd, P. W., Jickells, T., Law, C. S., Blain, S., Boyle, E. A., Buesseler, K. O., *Coale, K. H., Cullen, J. J., Baar, H. J. W. de, Follows, M., Harvey, M., Lancelot, C., Levasseur, M., Owens, N. P. J., Pollard, R., Rivkin, R. B., Sarmiento, J., Schoemann, V., Smetacek, V., Takeda, S., Tsuda, A., Turner, S., and Watson, A. J.*: Mesoscale Iron Enrichment Experiments 1993–2005: Synthesis and Future Directions. *Science*, 315, 612–617, https://doi.org/10.1126/science.1131669, 2007.

Deleted: et al. (2007)....oale, K. H., Cullen, J. J., Baar, H. J. W. de, Follows, M., Harvey, M., Lancelot, C., Levasseur, M., Owens, N. P. J., Pollard, R., Rivkin, R. B., Sarmiento, J., Schoemann, V., Smetacek, V., Takeda, S., Tsuda, A., Turner, S., and Watson, A. J.: Mesoscale Iron Enrichment Experiments 1993–2005: Synthesis and Future Directions.... *Science*, 315(5812),..., 612–617. (... [125])

16589 Cape, M. R., Vernet, M., Pettit, E. C., Wellner, J., Truffer, M., Akie, G., *Domack, E., Leventer, A., Smith, C. R., and Huber, B. A.*: Circumpolar Deep Water Impacts Glacial Meltwater Export and Coastal Biogeochemical Cycling Along the West Antarctic Peninsula. *Front. Mar. Sci.*, 6, 16590 16591 https://doi.org/10.3389/fmars.2019.00144, 2019.

Deleted: et al. (2019)....omack, E., Leventer, A., Smith, C. R., and Huber, B. A.: Circumpolar Deep Water Impacts Glacial Meltwater Export and Coastal Biogeochemical Cycling Along the West Antarctic Peninsula. *Frontiers in Marine Science*, 6. (... [126])

16593 Cavalieri, D., Parkinson, C., Gloersen, P., *and* Zwally, H. J.: Sea Ice Concentrations from 16594 Nimbus-7 SMMR and DMSP SSM/I-SSMIS Passive Microwave Data, Version 1. 16595 https://doi.org/10.5067/8GQ8LZQL0VL, 1996.

Deleted: &...nd Zwally, H. J. (1996)....: Sea Ice Concentrations from Nimbus-7 SMMR and DMSP SSM/I-SSMIS Passive Microwave Data, Version 1 [Data set]. NASA National Snow and Ice Data Center DAAC. (... [127])

16596 Death, R., Wadham, J. L., Monteiro, F., Le Brocq, A. M., Tranter, M., Ridgwell, A., *Dutkiewicz, S., and Raiswell, R.*: Antarctic ice sheet fertilises the Southern Ocean. *BG*, 11, 2635–2643, 16597 16598 https://doi.org/10.5194/bg-11-2635-2014, 2014.

Deleted: et al. (2014)....utkiewicz, S., and Raiswell, R.: Antarctic ice sheet fertilises the Southern Ocean. *Biogeosciences*... *BG*, 11(10),..., 2635–2643. (... [128])

16599 Dinniman, M. S., St-Laurent, P., Arrigo, K. R., Hofmann, E. E., *and* Dijken, G. L.: Analysis of 16600 Iron Sources in Antarctic Continental Shelf Waters. *J. Geophys. Res. Oceans*, 125, 16601 https://doi.org/10.1029/2019JC015736, 2020.

Deleted: & van...nd Dijken, G. L. (2020)....: Analysis of Iron Sources in Antarctic Continental Shelf Waters. *Journal of Geophysical Research:... J. Geophys. Res. Oceans*,..., 125(5).... (... [129])

16691 Dinniman, M. S., St-Laurent, P., Arrigo, K. R., Hofmann, E. E., and van Dijken, G. L.:
 16692 Sensitivity of the Relationship Between Antarctic Ice Shelves and Iron Supply to Projected
 16693 Changes in the Atmospheric Forcing. *J. Geophys. Res. Ocean.*, 128, e2022JC019210.
 16694 <https://doi.org/10.1029/2022JC019210>, 2023.

16695 Dotto, T. S., Naveira Garabato, A. C., Bacon, S., Holland, P. R., Kimura, S., Firing, Y. L.,
 16696 Tsamados, M., Wåhlin, A. K., and Jenkins, A.: Wind-Driven Processes Controlling Oceanic
 16697 Heat Delivery to the Amundsen Sea, Antarctica. *J. Phys. Oceanogr.*, 49, 2829–2849.
 16698 <https://doi.org/10.1175/JPO-D-19-0064.1>, 2019.

16699 Douglas, C. C., Briggs, N., Brown, P., MacGilchrist, G., and Naveira Garabato, A.: Exploring
 16700 the relationship between sea ice and phytoplankton growth in the Weddell Gyre using satellite
 16701 and Argo float data. *Ocean Sci.*, 20, 475–497, <https://doi.org/10.5194/os-20-475-2024>, 2024.

16702 Dutrieux, P., De Rydt, J., Jenkins, A., Holland, P. R., Ha, H. K., Lee, S. H., Steig, E. J., Ding,
 16703 Q., Abrahamsen, E. P., and Schröder, M.: Strong sensitivity of Pine Island ice-shelf melting to
 16704 climate variability. *Sci.*, 343, 6167, 174–178, DOI: 10.1126/science.1244341, 2014.

16705 ECCO Consortium, Fukumori, I., Wang, O., Fenty, I., Forget, G., Heimbach, P., and Ponte, R.
 16706 M: ECCO Ocean Mixed Layer Depth - Monthly Mean 0.5 Degree 9Version 4 Release 4). ver
 16707 V4r4, PO.DACC, CA, USA, Dataset accessed [2025-08-22], <https://doi.org/10.5067/ECG5M-OML44>, 2021.

16708 Forsch, K. O., Hahn-Woernle, L., Sherrell, R. M., Rocanova, V. J., Bu, K., Burdige, D., Vernet,
 16709 M., and Barbeau, K. A.: Seasonal dispersal of fjord meltwaters as an important source of iron
 16710 and manganese to coastal Antarctic phytoplankton. *Biogeo.*, 18, 6349–6375,
 16711 <https://doi.org/10.5194/bg-18-6349-2021>, 2021.

16712 Golder, M.R., and Antoine, D.: Physical drivers of long-term chlorophyll-a variability in the
 16713 Southern Ocean. *Elem. Sci Anth.*, 13:1, <https://doi.org/10.1525/elementa.2024.00077>, 2025.

16714 Garabato, A. C. N., Forryan, A., Dutrieux, P., Brannigan, L., Biddle, L. C., Heywood, K. J.,
 16715 Jenkins, A., Firing, Y. L., and Kimura, S.: Vigorous lateral export of the meltwater outflow from
 16716 beneath an Antarctic ice shelf. *Nature*, 542, 219–222, <https://doi.org/10.1038/nature20825>, 2017.

16717 Gerringsa, L. J. A., Alderkamp, A.-C., Laan, P., Thuróczy, C.-E., De Baar, H. J. W., Mills, M. M.,
 16718 van Dijken, G. L., Haren, H. van, and Arrigo, K. R.: Iron from melting glaciers fuels the
 16719 phytoplankton blooms in Amundsen Sea (Southern Ocean): Iron biogeochemistry. *Deep-Sea
 16720 Res.* II, 71–76, 16–31, <https://doi.org/10.1016/j.dsr2.2012.03.007>, 2012.

16721 Gerringsa, L. J. A., Alderkamp, A.-C., Laan, P., Thuróczy, C.-E., de Baar, H. J. W., Mills, M. M.,
 16722 van Dijken, G. L., van Haren, H., and Arrigo, K. R.: Corrigendum to “Iron from melting glaciers
 16723 fuels the phytoplankton blooms in Amundsen Sea (Southern Ocean): iron biogeochemistry”
 16724 (Gerringsa et al., 2012). *Deep-Sea Res.* II, 177, 104843.
 16725 <https://doi.org/10.1016/j.dsr2.2020.104843>, 2020.

Deleted: &
Deleted: . (2023).
Deleted: *Journal of Geophysical Research: Oceans*,
Deleted: (2),
Deleted: .
Deleted: . N
Deleted: et al. (2019).
Deleted: *Journal of Physical Oceanography*,
Deleted: (11),
Deleted: .

Formatted: Line spacing: single
Deleted: et al. (2012).
Deleted: .
Deleted: .
Deleted: Research Part
Deleted: : *Topical Studies in Oceanography*,
Deleted: .
Deleted: et al. (2020).
Deleted:).
Deleted: .
Deleted: Research Part
Deleted: : *Topical Studies in Oceanography*,
Deleted: .

16827 Huang, B., Liu, C., Banzon, V., Freeman, E., Graham, G., Hankins, B., Smith, T., and Zhang, H.-M.: Improvements of the Daily Optimum Interpolation Sea Surface Temperature (DOISST) Version 2.1, *Journal of Climate*, 34, 2923–2939. doi: 10.1175/JCLI-D-20-0166.1, 2021.

16831 Jacobs, S. S., Jenkins, A., Giulivi, C. F., and Dutrieux, P.: Stronger ocean circulation and
16832 increased melting under Pine Island Glacier ice shelf, *Nat. Geo.*, 4, 519–523.
16833 https://doi.org/10.1038/ngeo1188, 2011.

16834 Jena, B. and Pillai, A. N.: Satellite observations of unprecedented phytoplankton blooms in the
16835 Maud Rise polynya, Southern Ocean, *The Cryosphere*, 14, 1385–1398.
16836 https://doi.org/10.5194/tc-14-1385-2020, 2020.

16837 Jenkins, A., Dutrieux, P., Jacobs, S. S., McPhail, S. D., Perrett, J. R., Webb, A. T., and White,
16838 D.: Observations beneath Pine Island glacier in West Antarctica and implications for its retreat,
16839 *Nat. Geo.*, 3, 468–472, https://doi.org/10.1038/NGEO890, 2010.

16840 Jourdain, N. C., Mathiot, P., Merino, N., Durand, G., Le Sommer, J., Spence, P., Dutrieux, P.,
16841 and Madec, G.: Ocean circulation and sea-ice thinning induced by melting ice shelves in the
16842 Amundsen Sea, *J. Geophys. Res. Ocean.*, 122, 2550–2573.
16843 https://doi.org/10.1002/2016JC012509, 2017.

16844 Kauko, H. M., Hattermann, T., Ryan-Keogh, T., Singh, A., de Steur, L., Fransson, A., Chierici,
16845 M., Falkenhaug, T., Halffredsson, E. H., Bratbak, G., Tsagaraki, T., Berge, T., Zhou, Q., and
16846 Moreau, S.: Phenology and Environmental Control of Phytoplankton Blooms in the Kong Håkon
16847 VII Hav in the Southern Ocean, *Front. Mar. Sci.*, 8, https://doi.org/10.3389/fmars.2021.623856,
16848 2021.

16849 Lannuzel, D., Fourquez, M., de Jong, J., Tison, J.-L., Delille, B., and Schoemann, V.: First report
16850 on biological iron uptake in the Antarctic sea-ice environment, *Polar Biol.*, 46, 339–355.
16851 https://doi.org/10.1007/s00300-023-03127-7, 2023.

16852 Lee, S. H., Kim, B. K., Lim, Y. J., Joo, H., Kang, J. J., Lee, D., Park, J., Ha, S.-Y., and Lee, S.
16853 H.: Small phytoplankton contribution to the standing stocks and the total primary production in
16854 the Amundsen Sea, *BG*, 14, 3705–3713, https://doi.org/10.5194/bg-14-3705-2017, 2017.

16855 Lee, Y., Park, J., Jung, J., and Kim, T. W.: Unprecedented differences in phytoplankton
16856 community structures in the Amundsen Sea polynyas, West Antarctica, *Environ. Res. Lett.* 17,
16857 114022, 10.1088/1748-9326/ac9a5f, 2022.

16858 van Leeuwe, M. A., Webb, A. L., Venables, H. J., Visser, R. J. W., Meredith, M. P., Elzenga J.
16859 T. M., and Stefels, J.: Annual patterns in phytoplankton phenology in Antarctic coastal waters
16860 explained by environmental drivers, *Limnol. Oceanogr.*, 65, 1651–1668.
16861 https://doi.org/10.1002/lno.11477, 2020.

16862 Liniger, G., Strutton, P. G., Lannuzel, D., and Moreau, S.: Calving event led to changes in
16863 phytoplankton bloom phenology in the Mertz polynya, Antarctica, *J. Geophys. Res. Oceans.*,
16864 125, e2020JC016387, https://doi.org/10.1029/2020JC016387, 2020.

Deleted: &
Deleted: (2011).
Deleted: . *Nature Geoscience*,
Deleted: (8),
Deleted: .

Formatted: Normal, Line spacing: single
Deleted: et al. (2017).

Deleted: . *Journal of Geophysical Research: Oceans*,
Deleted: (3),
Deleted: .
Deleted: et al. (2021).

Deleted: . *Frontiers in Marine Science*, 8.
https://doi.org/10.3389/fmars.2021.623856

Deleted: &
Deleted: (2023).
Deleted: .
Deleted: *Biology*
Deleted: (4),
Deleted: .
Deleted: Biogeosciences

16888
16889 Liu, Y., Moore, J. C., Cheng, X., Gladstone, R. M., Bassis, J. N., Liu, H., [Wen, J., and Hui, F.](#):
16890 Ocean-driven thinning enhances iceberg calving and retreat of Antarctic ice shelves, *Proc. Nat.*
16891 *Acad. Sci.*, 112, 3263–3268, <https://doi.org/10.1073/pnas.1415137112>, 2015.

16892
16893 van Manen, M., Aoki, S., Brussaard, C. P. D., Conway, T. M., Eich, C., Gerrings, L., Jung, J.,
16894 Kim, T.-W., Lee, S. H., Lee, Y., Reichart, G.-J., Tian, H., Wille, F., and Middag, R.: The role of
16895 the Dotson Ice Shelf and circumpolar deep water as driver and source of dissolved and
16896 particulate iron and manganese in the Amundsen Sea polynya, *Southern Ocean, Mar. Chem.*,
16897 104161, <https://doi.org/10.1016/j.marchem.2022.104161>, 2022.

16898 Marchese, C., Albouy, C., Tremblay, J.-É., Dumont, D., D'Ortenzio, F., Vissault, S., [and](#)
16899 Bélanger, S.: Changes in phytoplankton bloom phenology over the North Water (NOW)
16900 polynya: a response to changing environmental conditions, *Polar Biol.*, 40, 1721–1737,
16901 <https://doi.org/10.1007/s00300-017-2095-2>, 2017.

16902 [Maritorena, S., and Siegel, D. A.: Consistent merging of satellite ocean color data sets using a](#)
16903 [bio-optical model, Rem. Sens. Environ.](#), 94, 429–440, <https://doi.org/10.1016/j.rse.2004.08.014>,
16904 2005.

16905
16906 [McClish, S., and Bushinsky, S. M.: Majority of Southern Ocean seasonal ice zone bloom net](#)
16907 [community production precedes total ice retreat, Geophys. Res. Lett.](#), 50, e2023GL103459,
16908 <https://doi.org/10.1029/2023GL103459>, 2023.

16909
16910 Meredith, M., Sommerkorn, [M.](#), Cassotta, [S.](#), Derksen, [C.](#), Ekyaykin, [A.](#), Hollowed, [A.](#), Kofinas, [G.](#),
16911 Mackintosh, [A.](#), Melbourne-Thomas, [J.](#), Muelbert, [M.M.C.](#), Ottersen, [G.](#), Pritchard, [H.](#), and
16912 Schurr, [E.A.G.](#): Polar Regions. In: *IPCC Special Report on the Ocean and Cryosphere in a*
16913 *Changing Climate* [H.-O. Pörtner, D.C. Roberts, V. Masson-Delmotte, P. Zhai, M. Tignor, E.
16914 *Poloczanska, K. Mintenbeck, A. Alegria, M. Nicolai, A. Okem, J. Petzold, B. Rama, N.M.*
16915 *Weyer (eds.)]. Cambridge University Press, Cambridge, UK and New York, NY, USA, pp. 203–*
16916 [320. https://doi.org/10.1017/9781009157964.005](https://doi.org/10.1017/9781009157964.005), 2019.

16917 [Mills, M. M., Lindsey, R.K., van Dijken, G. L., Alderkamp, C-A., Berg, G. M., Robinson, D. H.,](#)
16918 [Welschmeyer, N. A and Arrigo, K. R.: Photophysiology in two Southern Ocean phytoplankton](#)
16919 [taxa: photosynthesis of *phaeocystis antarctica* \(prymnesiophyceae\) and *fragilariaopsis cylindrus*](#)
16920 [\(bacillariophyceae\) under simulated mixed-layer irradiance, J. Phycol.](#), 46, 1114–1127,
16921 <https://doi.org/10.1111/j.1529-8817.2010.00923.x>, 2010.

16922 [Mills, M. M., Alderkamp, C-A., Thuróczy, C-E., van Dijken, G. L., Laan, P., de Barr, H. J. W.](#)
16923 [and Arrigo, K. R.: Phytoplankton biomass and pigment responses to Fe amendments on the Pine](#)
16924 [Island and Amundsen polynyas, Deep-Sea Res. II.](#), 71–76, 61–76,
16925 <https://doi.org/10.1016/j.dsr2.2012.03.008>, 2012.

16926 [Morales Maqueda, M. A.: Polynya Dynamics: a Review of Observations and Modeling, Rev.](#)
16927 [Geophys.](#), 42, RG1004, <https://doi.org/10.1029/2002RG000116>, 2004.

Deleted: et al. (2015).
Formatted: Normal, Line spacing: single
Deleted: *Proceedings of the National Academy of Sciences*,
Deleted: (11),
Deleted: <https://doi.org/10.1073/pnas.1415137112>

Deleted: &
Formatted: Line spacing: single
Deleted: . (2017).
Deleted: .
Deleted: *Biology*
Deleted: (9),
Deleted: .

Deleted: M.
Deleted: S.
Formatted: Line spacing: single
Deleted: C.
Deleted: A.
Deleted: .
Deleted: G.
Deleted: A.
Deleted: J.
Deleted: M.M.C.
Deleted: G.
Deleted: H.
Deleted: . Schuur, 2019.
Deleted: .

Deleted: . (2004).
Deleted: *Reviews of Geophysics*,
Formatted: Line spacing: single
Deleted: (1),
Deleted: .

16955 Moreau, S., Mostajir, B., Bélanger, S., Schloss, I. R., Vancoppenolle, M., Demers, S., **and**
 16956 Ferreyra, G. A.: Climate change enhances primary production in the western Antarctic Peninsula,
 16957 Global Change Biology, 21, 2191–2205, <https://doi.org/10.1111/gcb.12878>, 2015. **Deleted:** &...nd Ferreyra, G. A. (2015)....: Climate change
 enhances primary production in the western Antarctic Peninsula.... Global Change Biology, 21(6),... 2191-... [130]

16958 Naughten, K. A., Holland, P. R., and De Rydt, J.: Unavoidable future increase in West Antarctic
 16959 ice-shelf melting over the twenty-first century, Nat. Clim. Change., 13, 1222–1228,
 16960 <https://doi.org/10.1038/s41558-023-01818-x>, 2023.

16961 Naughten, K. A., Meissner, K. J., Galton-Fenzi, B. K., England, M. H., Timmermann, R., **and**
 16962 Hellmer, H. H.: Future Projections of Antarctic Ice Shelf Melting Based on CMIP5 Scenarios, J.
 16963 Clim., 31, 5243–5261, <https://doi.org/10.1175/JCLI-D-17-0854.1>, 2018. **Deleted:** &...nd Hellmer, H. H. (2018)....: Future
 Projections of Antarctic Ice Shelf Melting Based on CMIP5 Scenarios. *Journal of Climate*,... J. Clim., 31(13),... 5243–
 5261.... [131]

16964 Nunes, G.S., Ferreira, A. and Brito, A.C. Long-term satellite data reveals complex phytoplankton
 16965 dynamics in the Ross Sea, Antarctica. Commun. Earth. Environ., 6, 864.
 16966 <https://doi.org/10.1038/s43247-025-02590-w>, 2025. **Formatted:** Line spacing: single
Deleted: Naveira Garabato, A. C. N., Forryan, A., Dutrieux, P., Brannigan, L., Biddle, L. C., Heywood, K. J., et al. (2017). Vigorous lateral export of the meltwater outflow from beneath an Antarctic ice shelf. *Nature*, 542(7640), 219–222. <https://doi.org/10.1038/nature20825>

16967 Oh, J.-H., Noh, K. M., Lim, H.-G., Jin, E. K., Jun, S.-Y., **and** Kug, J.-S.: Antarctic meltwater-
 16968 induced dynamical changes in phytoplankton in the Southern Ocean, Environ. Res. Lett., 17,
 16969 024022, <https://doi.org/10.1088/1748-9326/ac444e>, 2022. **Formatted:** Normal, Line spacing: single
Deleted: &...nd Kug, J.-S. (2022)....: Antarctic meltwater-induced dynamical changes in phytoplankton in the Southern Ocean. *Environmental Research Letters*,... Environ. Res. Lett., 17(2),... 024022. [132]

16970 Oliver, H., St-Laurent, P., Sherrell, R. M., **and** Yager, P. L.: Modeling Iron and Light Controls
 16971 on the Summer *Phaeocystis antarctica* Bloom in the Amundsen Sea Polynya, Global
 16972 *Biogeochem.* Cycles, 2018GB006168, <https://doi.org/10.1029/2018GB006168>, 2019. **Deleted:** &...nd Yager, P. L. (2019)....: Modeling Iron and Light Controls on the Summer *Phaeocystis antarctica* Bloom in the Amundsen Sea Polynya.... Global *Biogeochemical...iogeochem.* Cycles, 2018GB006168, 2019. [133]

16973 Pan, J. B., Gierach, M. M., Stammerjohn, S., Schofield, O., Meredith, M. P., Reynolds, R. A.,
 16974 vernet, M., Haumann, F. A., **Orona, A. J., and Miller, C. E.**: Impact of glacial meltwater on
 16975 phytoplankton biomass along the Western Antarctic Peninsula. *Comm. Earth. Environ.*, 6(456).
 16976 <https://doi.org/10.1038/s43247-025-02435-6>, 2025. **Deleted:** et al. (2025)...rona, A. J., and Miller, C. E.: Impact of glacial meltwater...eltwater on phytoplankton...hytoplankton biomass along the Western Antarctic Peninsula. *Communication...omm. Earth & Environment*,... [134]

16977 Paolo, F. S., Fricker, H. A., **and** Padman, L.: Volume loss from Antarctic ice shelves is
 16978 accelerating, Science, 348, 327–331, <https://doi.org/10.1126/science.aaa0940>, 2015. **Deleted:** &...nd Padman, L. (2015)....: Volume loss from Antarctic ice shelves is accelerating.... Science, 348(6232),... 327–331. [135]

16979 Paolo, F. S., Fricker, H. A., **and** Padman, L.: Constructing improved decadal records of Antarctic
 16980 ice shelf height change from multiple satellite radar altimeters, Remote *Sens. Environ.* 177, 192–
 16981 205, <https://doi.org/10.1016/j.rse.2016.01.026>, 2016. **Deleted:** &...nd Padman, L. (2016)....: Constructing improved decadal records of Antarctic ice shelf height change from multiple satellite radar altimeters.... Remote *Sensing of Environment*,...ens. Environ. 177, 192–205. [136]

16982 Paolo, F. S., Gardner, A. S., Greene, C. A., Nilsson, J., Schodlok, M. P., Schlegel, N.-J., **and**
 16983 Fricker, H. A.: Widespread slowdown in thinning rates of West Antarctic ice shelves, *TC*, 17,
 16984 3409–3433, <https://doi.org/10.5194/tc-17-3409-2023>, 2023. **Deleted:** &...nd Fricker, H. A. (2023)....: Widespread slowdown in thinning rates of West Antarctic ice shelves. *The Cryosphere*,... TC, 17(8),... 3409–3433. [137]

16985 Park, J., Kuzminov, F. I., Bailleul, B., Yang, E. J., Lee, S., Falkowski, P. G., **and** Gorbunov, M.
 16986 Y.: Light availability rather than Fe controls the magnitude of massive phytoplankton bloom in
 16987 the Amundsen Sea polynyas, Antarctica, **Light availability rather than Fe controls phytoplankton**
 16988 **bloom**, *Limnol. Oceanogr.*, 62, 2260–2276, <https://doi.org/10.1002/lo.10565>, 2017. **Deleted:** Park, J., Kim, J.-H., Kim, H., Hwang, J., Jo, Y.-H., & Lee, S. H. (2019). Environmental Forcings on the Remotely Sensed Phytoplankton Bloom Phenology in the Central Ross Sea Polynya. *Journal of Geophysical Research: Oceans*, 124(8), 5400–5417. <https://doi.org/10.1029/2019JC015222> [138]

16989 Park, J., Kim, J.-H., Kim, H., Hwang, J., Jo, Y.-H., and Lee, S. H.: Environmental Forcings on
 16990 the Remotely Sensed Phytoplankton Bloom Phenology in the Central Ross Sea Polynya, J.
 16991 Geophys. Res. Ocean., 124, 5400–5417, <https://doi.org/10.1029/2019JC015222>, 2019.

17090 Person, R., Aumont, O., Madec, G., Vancoppenolle, M., Bopp, L., and Merino, N.: Sensitivity of
17091 ocean biogeochemistry to the iron supply from the Antarctic Ice Sheet explored with a
17092 biogeochemical model. *BG*, 16, 3583–3603. <https://doi.org/10.5194/bg-16-3583-2019>, 2019.

17093 Pritchard, H. D., Ligtenberg, S. R. M., Fricker, H. A., Vaughan, D. G., van den Broeke, M. R.,
17094 and Padman, L.: Antarctic ice-sheet loss driven by basal melting of ice shelves. *Nat.*, 484, 502–
17095 505. <https://doi.org/10.1038/nature10968>, 2012.

17096 Racault, M.-F., Le Quéré, C., Buitenhuis, E., Sathyendranath, S., and Platt, T.: Phytoplankton
17097 phenology in the global ocean. *Ecol. Indic.*, 14, 152–163.
17098 <https://doi.org/10.1016/j.ecolind.2011.07.010>, 2012.

17099 Randall-Goodwin, E., Meredith, M. P., Jenkins, A., Yager, P. L., Sherrell, R. M., Abrahamsen,
17100 E. P., Guerrero, R., Yuan, X., Mortlock, R. A., Gavahan, K., Alderkamp, A.-C., Ducklow, H.,
17101 Robertson, R., and Stammerjohn, S. E.: Freshwater distributions and water mass structure in the
17102 Amundsen Sea Polynya region, Antarctica. *Elem. Sci. Anth.*, 3, 000065.
17103 <https://doi.org/10.12952/journal.elementa.000065>, 2015.

17104 Rignot, E., Jacobs, S., Mouginot, J., and Scheuchl, B.: Ice-Shelf Melting Around Antarctica. *Sci.*,
17105 341, 266–270. <https://doi.org/10.1126/science.1235798>, 2013.

17106 Rignot, E., Mouginot, J., Scheuchl, B., van den Broeke, M., van Wessem, M. J., and Morlighem,
17107 M.: Four decades of Antarctic Ice Sheet mass balance from 1979–2017. *Proc. Nat. Acad. Sci.*,
17108 116, 4, 1095–1103. <https://doi.org/10.1073/pnas.1812883116>, 2019.

17109 Ryan-Keogh, T. J., Thomalla, S. J., Chang, N., and Moalusi, T.: A new global oceanic multi-
17110 model net primary productivity data product. *Earth Syst. Sci. Data*, 15, 4829–4848.
17111 <https://doi.org/10.5194/essd-15-4829-2023>, 2023.

17112 Sari El Dine, Z., Guinet, C., Picard, B., Thyssen, M., Duforêt-gaurier, L., and El Hourany,
17113 R.: Influence of the phytoplankton community structure on the southern elephant seals' foraging
17114 activity within the Southern Ocean. *Commun. Biol.*, 8, 620. [https://doi.org/10.1038/s42003-025-08049-0](https://doi.org/10.1038/s42003-025-
17115 08049-0), 2025.

17116 Scambos, T., Bell, R. E., Alley, R. B., Anandakrishnan, S., Bromwich, D. H., Brunt, K.,
17117 Christianson, K., Creyts, T., Das, S. B., DeConto, R., Dutrieux, P., Fricker, H. A., Holland, D.,
17118 MacGregor, J., Medley, B., Nicolas, J. P., Pollard, D., Siegfried, M. R., Smith, A. M., Steig, E.,
17119 J., Trusel, L. D., Vaughan, D. G., and Yager, P. L.: How much, how fast?: A science review and
17120 outlook for research on the instability of Antarctica's Thwaites Glacier in the 21st century. *Glob.*
17121 *Planet. Change.*, 153, 16–34. <https://doi.org/10.1016/j.gloplacha.2017.04.008>, 2017.

17122 Silsbe, G. M., Behrenfeld, M. J., Halsey, K. H., Milligan, A. J., and Westberry, T. K.: The CAFE
17123 model: A net production model for global ocean phytoplankton. *Global Biogeochem. Cycles*,
17124 30, 1756–1777. [doi:10.1002/2016GB005521](https://doi.org/10.1002/2016GB005521), 2016.

17125 Shepherd, A., Ivins, E., Rignot, E., Smith, B., van den Broeke, M., Velicogna, I., Whitehouse, P.,
17126 Briggs, K., Joughin, I., Krinner, G., Nowicki, S., Payne, T., Scambos, T., Schlegel, N., A. G.,
17127 <https://doi.org/10.1016/j.gloplacha.2017.04.008>, 2018.

17128 Deleted: &
17129 Deleted: . (2019).
17130 Formatted: Line spacing: single
17131 Deleted: . *Biogeosciences*
17132 Deleted: (18),
17133 Deleted: .
17134 Deleted: &
17135 Deleted: . (2012).
17136 Deleted: . *Nature*,
17137 Deleted: (7395).
17138 Deleted: .
17139 Deleted: &
17140 Deleted: . (2012).
17141 Deleted: . *Ecological Indicators*,
17142 Deleted: (1).
17143 Deleted: .
17144 Deleted: et al. (2015).
17145 Deleted: . *Elementa: Science of the Anthropocene*,
17146 Deleted: .
17147 Deleted: &
17148 Deleted: . (2013).
17149 Deleted: . *Science*
17150 Deleted: (6143).
17151 Deleted: .
17152 Deleted: &
17153 Deleted: . (2019).
17154 Deleted: . *Proceedings of the National Academy of Sciences*,
17155 Deleted: ().
17156 Deleted:).
17157 Deleted: . <https://doi.org/10.1073/pnas.1812883116>

17160 Agosta, C., Ahlström, A., Babonis, G., Barletta, V., Blazquez, A., Bonin, J., Csatho, B.,
17161 Cullather, R., Felikson, D., Fettweis, X., Forsberg, R., Gallee, H., Gardner, A., Gilbert, L., Groh,
17162 A., Gunter, B., Hanna, E., Harig, C., Helm, V., Horvath, A., Horwath, M., Khan, S., Kjeldsen, K.,
17163 K., Konrad, H., Langen, P., Lecavalier, B., Loomis, B., Luthcke, S., McMillan, M., Melini, D.,
17164 Mernild, S., Mohajerani, Y., Moore, P., Mouginot, J., Moyano, G., Muir, A., Nagler, T., Nield,
17165 G., Nilsson, J., Noel, B., Otosaka, I., Pattle, M. E., Peltier, W. R., Pie, N., Rietbroek, R., Rott, H.,
17166 Sandberg-Sørensen, L., Sasgen, I., Save, H., Scheuchl, B., Schrama, E., Schröder, L., Seo, K.-
17167 W., Simonsen, S., Slater, T., Spada, G., Suterley, T., Talpe, M., Tarasov, L., van de Berg, W. J.,
17168 van der Wal, W., van Wessem, M., Vishwakarma, B. D., Wiese, D., Wouters, B., and The
17169 IMBIE team: Mass balance of the Antarctic Ice Sheet from 1992 to 2017. *Nat.*, 558, 219–222.
17170 <https://doi.org/10.1038/s41586-018-0179-y>, 2018.

Deleted: *Nature*, ... *Nat.*, 558(7709), ... 219–222. ... [139]

17171 Sherrell, R. M., Lagerström, M. E., Forsch, K. O., Stammerjohn, S. E., and Yager, P. L.:
17172 Dynamics of dissolved iron and other bioactive trace metals (Mn, Ni, Cu, Zn) in the Amundsen
17173 Sea Polynya, Antarctica. *Elementa: Sci. Anthropol.*, 3, 000071.
17174 <https://doi.org/10.12952/journal.elementa.000071>, 2015.

Deleted: &...nd Yager, P. L. (2015)...: Dynamics of dissolved iron and other bioactive trace metals (Mn, Ni, Cu, Zn) in the Amundsen Sea Polynya, Antarctica.... *Elementa*, ... *Sci. Anthropol.*, 3, 000071. ... [140]

17175 Siegel, D. A., Doney, S. C., and Yoder, J. A.: The North Atlantic Spring Phytoplankton Bloom
17176 and Sverdrup's Critical Depth Hypothesis. *Science*, 296, 730–733.
17177 <https://doi.org/10.1126/science.1069174>, 2002.

Deleted: &...nd Yoder, J. A. (2002)...: The North Atlantic Spring Phytoplankton Bloom and Sverdrup's Critical Depth Hypothesis.... *Science*, 296(5568), ... 730–733. ... [141]

17178 Smith, A. J. R., Nelson, T., Ratnarajah, L., Genovese, C., Westwood, K., Holmes, T. M., Corkill,
17179 M., Townsend, A. T., Bell, E., Wuttig, K., and Lannuzel, D.: Identifying potential sources of
17180 iron-binding ligands in coastal Antarctic environments and the wider Southern Ocean. *Front. Mar. Sci.*, 9, <https://doi.org/10.3389/fmars.2022.948772>, 2022.

Deleted: et al. (2022)...orkill, M., Townsend, A. T., Bell, E., Wuttig, K., and Lannuzel, D.: Identifying potential sources of iron-binding ligands in coastal Antarctic environments and the wider Southern Ocean. *Frontiers in Marine Science*, 9. ... [142]

17182 Soppa, M. A., Völker, C., and Bracher, A.: Diatom Phenology in the Southern Ocean: Mean
17183 Patterns, Trends and the Role of Climate Oscillations. *Remote Sens.*, 8, 420.
17184 <https://doi.org/10.3390/rs8050420>, 2016.

Deleted: &...nd Bracher, A. (2016)...: Diatom Phenology in the Southern Ocean: Mean Patterns, Trends and the Role of Climate Oscillations.... *Remote Sensing*, 8(5) ... [143]

17185 Stammerjohn, S. E., Martinson, D. G., Smith, R. C., and Iannuzzi, R. A.: Sea ice in the western
17186 Antarctic Peninsula region: Spatio-temporal variability from ecological and climate change
17187 perspectives. *Deep-Sea Res. II*, 55, 2041–2058. <https://doi.org/10.1016/j.dsr2.2008.04.026>,
17188 2008.

Deleted: &...nd Iannuzzi, R. A. (2008)...: Sea ice in the western Antarctic Peninsula region: Spatio-temporal variability from ecological and climate change perspectives.... *Deep ...Sea Research Part...es. II: Topical Studies in Oceanography*, ... 55(18–19), ... 2041–205 ... [144]

17189 Stoer, A. C., and Fennel, K.: Carbon-centric dynamics of Earth's marine phytoplankton. *Proc. Nat. Acad. Sci.*, 121, 45, e2405354121, <https://doi.org/10.1073/pnas.2405354121>
17190 . 2024.

Deleted: &...nd Dinniman, M. S. (2017)...: Pathways and supply of dissolved iron in the Amundsen Sea (Antarctica). *Journal of Geophysical Research: ..., J. Geophys. Res. Oceans*, ... 122(9), ... 7135–7162. ... [145]

17193 St-Laurent, P., Yager, P. L., Sherrell, R. M., Stammerjohn, S. E., and Dinniman, M. S.: Pathways*
17194 and supply of dissolved iron in the Amundsen Sea (Antarctica). *J. Geophys. Res. Oceans*, 122,
17195 7135–7162. <https://doi.org/10.1002/2017JC013162>, 2017.

Deleted: &...nd Dinniman, M. S. (2017)...: Pathways and supply of dissolved iron in the Amundsen Sea (Antarctica). *Journal of Geophysical Research: ..., J. Geophys. Res. Oceans*, ... 122(9), ... 7135–7162. ... [145]

17196 St-Laurent, P., Yager, P. L., Sherrell, R. M., Oliver, H., Dinniman, M. S., and Stammerjohn, S.
17197 E.: Modeling the Seasonal Cycle of Iron and Carbon Fluxes in the Amundsen Sea Polynya,
17198 Antarctica. *J. Geophys. Res. Oceans*, 124, 1544–1565. <https://doi.org/10.1029/2018JC014773>,
17199 2019.

Deleted: &...nd Stammerjohn, S. E. (2019)...: Modeling the Seasonal Cycle of Iron and Carbon Fluxes in the Amundsen Sea Polynya, Antarctica. *Journal of Geophysical Research: ..., J. Geophys. Res. Oceans*, ... 124(3), ... 1544–1565. ... [146]

17293 Tagliabue, A., Bowie, A. R., DeVries, T., Ellwood, M. J., Landing, W. M., Milne, A., [Ohnemus, D. C., Twining, B. S., and Boyd, P. W.](#): The interplay between regeneration and scavenging fluxes drives ocean iron cycling. *Nat Commun*, 10, 4960, <https://doi.org/10.1038/s41467-019-12775-5>, 2019. **Deleted:** et al. (2019)...hnemus, D. C., Twining, B. S., and Boyd, P. W.: The interplay between regeneration and scavenging fluxes drives ocean iron cycling. *Nature Communications*... *Nat Commun*, 10(1), 4960. ... [147]

17297 Tamsitt, V., England, M. H., Rintoul, S. R., [and Morrison, A. K.](#): Residence Time and Transformation of Warm Circumpolar Deep Water on the Antarctic Continental Shelf. *Geophys. Res. Lett.*, 48, e2021GL096092, <https://doi.org/10.1029/2021GL096092>, 2021. **Deleted:** &...nd Morrison, A. K. (2021)...: Residence Time and Transformation of Warm Circumpolar Deep Water on the Antarctic Continental Shelf. *Geophysical Research Letters*... *Geophys. Res. Lett.*, 48(20), e2021GL096092. ... [148]

17300 Tamura, T. P., Nomura, D., Hirano, D., Tamura, T., Kiuchi, M., Hashida, G., [Makabe, R., Ono, K., Ushio, S., Yamazaki, K., Nakayama, Y., Takahashi, K. D., Sasaki, H., Murase, H., and Aoki, S.](#): Impacts of basal melting of the Totten Ice Shelf and biological productivity on marine biogeochemical components in Sabrina Coast, East Antarctica. *Global Biogeochem. Cycles*, 37, e2022GB007510, <https://doi.org/10.1029/2022GB007510>, 2023. **Deleted:** et al. (2022)...akabe, R., Ono, K., Ushio, S., Yamazaki, K., Nakayama, Y., Takahashi, K. D., Sasaki, H., Murase, H., and Aoki, S.: Impacts of basal melting of the Totten Ice Shelf and biological productivity on marine biogeochemical components in Sabrina Coast, East Antarctica... *Global Biogeochemical...iogeochem. Cycles*, n/d(n/a), 37, e2022GB007510. ... [149]

17305 [Thomalla, S.J., Nicholson, S.A., Ryan-Keogh, T.J. et al.](#) Widespread changes in Southern Ocean phytoplankton blooms linked to climate drivers. *Nat. Clim. Chang.* 13, 975–984, <https://doi.org/10.1038/s41558-023-01768-4>, 2023. **Deleted:** Thomalla, S. J., Ogunkoya, A. G., Vichi, M., & Swart, S. (2017). Using Optical Sensors on Gliders to Estimate Phytoplankton Carbon Concentrations and Chlorophyll-to-Carbon Ratios in the Southern Ocean. *Frontiers in Marine Science*, 4, <https://doi.org/10.3389/fmars.2017.00034>

17311 [Thuróczy, C.-E., Alderkamp, A.-C., Laan, P., Gerringa, L. J. A., Mills, M. M., van Dijken, G. L., De Baar, H. J. W., and Arrigo, K. R.](#): Key role of organic complexation of iron in sustaining phytoplankton blooms in the Pine Island and Amundsen Polynyas (Southern Ocean). *Deep-Sea Res. II*, 71–76, 49–60, <https://doi.org/10.1016/j.dsr2.2012.03.009>, 2012. **Formatted:** Line spacing: single

17312 Turner, J., Hosking, J. S., Marshall, G. J., Phillips, T., [and Bracegirdle, T. J.](#): Antarctic sea ice increase consistent with intrinsic variability of the Amundsen Sea Low. *Clim. Dyn.*, 46, 2391–2402, <https://doi.org/10.1007/s00382-015-2708-9>, 2016. **Deleted:** &...nd Bracegirdle, T. J. (2016)...: Antarctic sea ice increase consistent with intrinsic variability of the Amundsen Sea Low. *Climate Dynamics*... *Clim. Dyn.*, 46(7–8), 2391–2402. ... [150]

17315 [Vaillancourt, R. D., Sambrotto, R. N., Green, S., and Matsuda, A.](#): Phytoplankton biomass and photosynthetic competency in the summertime Mertz Glacier Region of East Antarctica. *Deep-Sea Res. II*, 50, 1415–1440, [https://doi.org/10.1016/S0967-0645\(03\)00077-8](https://doi.org/10.1016/S0967-0645(03)00077-8), 2003. **Deleted:** &...nd Matsuda, A. (2003)...: Phytoplankton biomass and photosynthetic competency in the summertime Mertz Glacier Region of East Antarctica... *Deep ...Sea Research Part...es. II: Topical Studies in Oceanography*..., 50(8–9), 1415–1440. ... [151]

17318 [Westberry, T., Behrenfeld, M. J., Siegel, D. A., and Boss, E.](#): Carbon-based primary productivity modeling with vertically resolved photoacclimation. *Global Biogeochem. Cycle.*, 22, GB2024, [doi:10.1029/2007GB003078](https://doi.org/10.1029/2007GB003078), 2008. **Deleted:** van Manen, M., Aoki, S., Brussaard, C. P. D., Conway, T. M., Eich, C., Gerringa, L. J. A., et al. (2022). The role of the Dotson Ice Shelf and circumpolar deep water as driver and source of dissolved and particulate iron and manganese in the Amundsen Sea polynya. *Southern Ocean. Marine Chemistry*, 104161. <https://doi.org/10.1016/j.marchem.2022.104161>

17321 [Yager, P. L., Sherrell, R. M., Stammerjohn, S., Alderkamp, A.-C., Schofield, O., Abrahamsen, P., Arrigo, K., Bertilsson, S., Garay, L., Guerrero, R., Lowry, K., Moksnes, P.-O., Ndungo, K., Post, A., Randall-Goodwin, E., Riemann, L., Severmann, S., Thatje, S., van Dijken, G., and Wilson, S.](#): ASPIRE: The Amundsen Sea Polynya International Research Expedition. *Oceanogr.*, 25, 40–53, <https://doi.org/10.5670/oceanog.2012.73>, 2012. **Deleted:** Stammerjohn, S. E..., Alderkamp, A.-C., Schofield, O., Abrahamsen, P., et al. (2012)...rrigo, K., Bertilsson, S., Garay, L., Guerrero, R., Lowry, K., Moksnes, P.-O., Ndungo, K., Post, A., Randall-Goodwin, E., Riemann, L., Severmann, S., Thatje, S., van Dijken, G., and Wilson, S.: ASPIRE: The Amundsen Sea Polynya International Research Expedition. *Oceanography*..., *Oceanogr.*, 25(3), 40–53. ... [153]

17327 [Yager P. L., Sherrell, R.M., Stammerjohn, S.E., Ducklow, H. W., Schofield, O., Ingall E.D., Wilson, S. E., Lowry, K. E., Willismd, C. M., Riemann, L., Bertilsson, S., Alderkamp, A-C., Dinasquet, J., Logares, R., Richert, I., Sipler, R. E., Melara A. J., Mu, L., Newstead, R. G., Post, A. F., Swalethorp, R and van Dijken, G. L.](#): A carbon budget for the Amundsen Sea Polynya, **Formatted:** Line spacing: single

17458 [Antarctica: Estimating net community production and export in a highly productive polar](#)
17459 [ecosystem, *Elem. Sci. Anth.*, 4, 000140, doi: 10.12952/journal.elementa.000140, 2016.](#)

17460 Yu, L.-S., He, H., Leng, H., Liu, H., [and](#) Lin, P.: Interannual variation of summer sea surface
17461 temperature in the Amundsen Sea, Antarctica, [Front. Mar. Sci.](#), 10,
17462 <https://doi.org/10.3389/fmars.2023.1050955>, 2023.

17463 Zheng, Y., Heywood, K. J., Webber, B. G. M., Stevens, D. P., Biddle, L. C., Bochme, L., [and](#)
17464 Loose, B.: Winter seal-based observations reveal glacial meltwater surfacing in the southeastern
17465 Amundsen Sea, [Commun. Earth Environ.](#), 2, 1–9, <https://doi.org/10.1038/s43247-021-00111-z>,
17466 2021.

17467 ▲

Deleted: &

Deleted: . (2023).

Formatted: Line spacing: single

Deleted: . *Frontiers in Marine Science*, 10.

Deleted: &

Deleted: . (2021).

Deleted: *Communications*

Deleted: & *Environment*,

Deleted: (1),

Deleted: .

Formatted: Font: +Headings CS (Times New Roman), 12
pt

Page 2: [1] Deleted	GL	11/12/25 3:03:00 PM
▼		
Page 6: [2] Deleted	GL	11/12/25 3:03:00 PM
▼		
Page 14: [3] Formatted	GL	11/12/25 3:03:00 PM
Font color: Auto		
Page 14: [4] Formatted	GL	11/12/25 3:03:00 PM
Line spacing: single		
Page 14: [5] Formatted Table	GL	11/12/25 3:03:00 PM
Formatted Table		
Page 14: [6] Formatted	GL	11/12/25 3:03:00 PM
Font color: Auto		
Page 14: [7] Formatted	GL	11/12/25 3:03:00 PM
Font color: Auto		
Page 14: [8] Formatted	GL	11/12/25 3:03:00 PM
Font color: Auto		
Page 14: [9] Formatted	GL	11/12/25 3:03:00 PM
Line spacing: single		
Page 14: [10] Formatted	GL	11/12/25 3:03:00 PM
Font color: Auto		
Page 14: [11] Formatted	GL	11/12/25 3:03:00 PM
Font color: Auto		
Page 14: [12] Formatted	GL	11/12/25 3:03:00 PM
Font color: Auto		
Page 14: [13] Formatted	GL	11/12/25 3:03:00 PM
Font color: Auto		
Page 14: [14] Formatted	GL	11/12/25 3:03:00 PM
Font color: Auto		
Page 14: [15] Formatted	GL	11/12/25 3:03:00 PM
Line spacing: single		
Page 14: [16] Formatted	GL	11/12/25 3:03:00 PM
Font color: Auto		
Page 14: [17] Formatted	GL	11/12/25 3:03:00 PM
Font color: Auto		
Page 14: [18] Formatted	GL	11/12/25 3:03:00 PM
Font color: Auto		

Page 14: [19] Formatted	GL	11/12/25 3:03:00 PM
Font color: Auto		
Page 14: [20] Formatted	GL	11/12/25 3:03:00 PM
Font color: Auto		
Page 14: [21] Formatted	GL	11/12/25 3:03:00 PM
Font color: Auto		
Page 14: [22] Formatted	GL	11/12/25 3:03:00 PM
Font color: Auto		
Page 14: [23] Formatted	GL	11/12/25 3:03:00 PM
Font color: Auto		
Page 14: [24] Formatted	GL	11/12/25 3:03:00 PM
Line spacing: single		
Page 14: [25] Formatted	GL	11/12/25 3:03:00 PM
Font color: Auto		
Page 14: [26] Formatted	GL	11/12/25 3:03:00 PM
Font color: Auto		
Page 14: [27] Formatted	GL	11/12/25 3:03:00 PM
Font color: Auto		
Page 14: [28] Formatted	GL	11/12/25 3:03:00 PM
Font color: Auto		
Page 14: [29] Formatted	GL	11/12/25 3:03:00 PM
Font color: Auto		
Page 14: [30] Formatted	GL	11/12/25 3:03:00 PM
Font color: Auto		
Page 14: [31] Formatted	GL	11/12/25 3:03:00 PM
Font color: Auto		
Page 14: [32] Formatted	GL	11/12/25 3:03:00 PM
Font color: Auto		
Page 14: [33] Formatted	GL	11/12/25 3:03:00 PM
Font color: Auto		
Page 14: [34] Formatted	GL	11/12/25 3:03:00 PM
Line spacing: single		
Page 14: [35] Formatted	GL	11/12/25 3:03:00 PM
Font color: Auto		
Page 14: [36] Formatted	GL	11/12/25 3:03:00 PM
Font color: Auto		

Page 14: [37] Formatted	GL	11/12/25 3:03:00 PM
Font color: Auto		
Page 14: [38] Formatted	GL	11/12/25 3:03:00 PM
Font color: Auto		
Page 14: [39] Formatted	GL	11/12/25 3:03:00 PM
Font color: Auto		
Page 14: [40] Formatted	GL	11/12/25 3:03:00 PM
Font color: Auto		
Page 14: [41] Formatted	GL	11/12/25 3:03:00 PM
Font color: Auto		
Page 14: [42] Formatted	GL	11/12/25 3:03:00 PM
Font color: Auto		
Page 14: [43] Formatted	GL	11/12/25 3:03:00 PM
Font color: Auto		
Page 14: [44] Formatted	GL	11/12/25 3:03:00 PM
Line spacing: single		
Page 14: [45] Formatted	GL	11/12/25 3:03:00 PM
Font color: Auto		
Page 14: [46] Formatted	GL	11/12/25 3:03:00 PM
Font color: Auto		
Page 14: [47] Formatted	GL	11/12/25 3:03:00 PM
Font color: Auto		
Page 14: [48] Formatted	GL	11/12/25 3:03:00 PM
Font color: Auto		
Page 14: [49] Formatted	GL	11/12/25 3:03:00 PM
Font color: Auto		
Page 14: [50] Formatted	GL	11/12/25 3:03:00 PM
Font color: Auto		
Page 14: [51] Formatted	GL	11/12/25 3:03:00 PM
Font color: Auto		
Page 14: [52] Formatted	GL	11/12/25 3:03:00 PM
Font color: Auto		
Page 14: [53] Formatted	GL	11/12/25 3:03:00 PM
Font color: Auto		
Page 14: [54] Formatted	GL	11/12/25 3:03:00 PM
Line spacing: single		

Page 14: [55] Formatted	GL	11/12/25 3:03:00 PM
Font color: Auto		
Page 14: [56] Formatted	GL	11/12/25 3:03:00 PM
Font color: Auto		
Page 14: [57] Formatted	GL	11/12/25 3:03:00 PM
Font color: Auto		
Page 14: [58] Formatted	GL	11/12/25 3:03:00 PM
Font color: Auto		
Page 14: [59] Formatted	GL	11/12/25 3:03:00 PM
Font color: Auto		
Page 14: [60] Formatted	GL	11/12/25 3:03:00 PM
Font color: Auto		
Page 14: [61] Formatted	GL	11/12/25 3:03:00 PM
Font color: Auto		
Page 14: [62] Formatted	GL	11/12/25 3:03:00 PM
Font color: Auto		
Page 14: [63] Formatted	GL	11/12/25 3:03:00 PM
Font color: Auto		
Page 14: [64] Formatted	GL	11/12/25 3:03:00 PM
Line spacing: single		
Page 14: [65] Formatted	GL	11/12/25 3:03:00 PM
Font color: Auto		
Page 14: [66] Formatted	GL	11/12/25 3:03:00 PM
Font color: Auto		
Page 14: [67] Formatted	GL	11/12/25 3:03:00 PM
Font color: Auto		
Page 14: [68] Formatted	GL	11/12/25 3:03:00 PM
Font: Not Bold, Font color: Auto		
Page 14: [69] Formatted	GL	11/12/25 3:03:00 PM
Font: Not Bold, Font color: Auto		
Page 14: [70] Formatted	GL	11/12/25 3:03:00 PM
Font color: Auto		
Page 14: [71] Formatted	GL	11/12/25 3:03:00 PM
Font color: Auto		
Page 14: [72] Formatted	GL	11/12/25 3:03:00 PM
Font color: Auto		

Page 14: [73] Formatted	GL	11/12/25 3:03:00 PM
Font color: Auto		
Page 14: [74] Formatted	GL	11/12/25 3:03:00 PM
Line spacing: single		
Page 14: [75] Formatted	GL	11/12/25 3:03:00 PM
Font color: Auto		
Page 14: [76] Formatted	GL	11/12/25 3:03:00 PM
Font: Not Bold, Font color: Auto		
Page 14: [77] Formatted	GL	11/12/25 3:03:00 PM
Font: Not Bold, Font color: Auto		
Page 14: [78] Formatted	GL	11/12/25 3:03:00 PM
Font: Not Bold, Font color: Auto		
Page 14: [79] Formatted	GL	11/12/25 3:03:00 PM
Font: Not Bold, Font color: Auto		
Page 14: [80] Formatted	GL	11/12/25 3:03:00 PM
Font color: Auto		
Page 14: [81] Formatted	GL	11/12/25 3:03:00 PM
Font color: Auto		
Page 14: [82] Formatted	GL	11/12/25 3:03:00 PM
Font color: Auto		
Page 14: [83] Formatted	GL	11/12/25 3:03:00 PM
Font color: Auto		
Page 14: [84] Formatted	GL	11/12/25 3:03:00 PM
Line spacing: single		
Page 14: [85] Formatted	GL	11/12/25 3:03:00 PM
Font color: Auto		
Page 14: [86] Formatted	GL	11/12/25 3:03:00 PM
Font color: Auto		
Page 14: [87] Formatted	GL	11/12/25 3:03:00 PM
Font color: Auto		
Page 14: [88] Formatted	GL	11/12/25 3:03:00 PM
Font color: Auto		
Page 14: [89] Formatted	GL	11/12/25 3:03:00 PM
Font color: Auto		
Page 14: [90] Formatted	GL	11/12/25 3:03:00 PM
Font color: Auto		

Page 14: [91] Formatted	GL	11/12/25 3:03:00 PM
Font color: Auto		
Page 14: [92] Formatted	GL	11/12/25 3:03:00 PM
Font color: Auto		
Page 14: [93] Formatted	GL	11/12/25 3:03:00 PM
Font color: Auto		
Page 14: [94] Formatted	GL	11/12/25 3:03:00 PM
Line spacing: single		
Page 14: [95] Formatted	GL	11/12/25 3:03:00 PM
Font color: Auto		
Page 14: [96] Formatted	GL	11/12/25 3:03:00 PM
Font color: Auto		
Page 14: [97] Formatted	GL	11/12/25 3:03:00 PM
Font color: Auto		
Page 14: [98] Formatted	GL	11/12/25 3:03:00 PM
Font: Not Bold, Font color: Auto		
Page 14: [99] Formatted	GL	11/12/25 3:03:00 PM
Font: Not Bold, Font color: Auto		
Page 14: [100] Formatted	GL	11/12/25 3:03:00 PM
Font color: Auto		
Page 14: [101] Formatted	GL	11/12/25 3:03:00 PM
Font color: Auto		
Page 14: [102] Formatted	GL	11/12/25 3:03:00 PM
Font color: Auto		
Page 14: [103] Formatted	GL	11/12/25 3:03:00 PM
Font color: Auto		
Page 14: [104] Formatted	GL	11/12/25 3:03:00 PM
Line spacing: single		
Page 14: [105] Formatted	GL	11/12/25 3:03:00 PM
Font color: Auto		
Page 14: [106] Formatted	GL	11/12/25 3:03:00 PM
Font color: Auto		
Page 14: [107] Formatted	GL	11/12/25 3:03:00 PM
Font color: Auto		
Page 14: [108] Formatted	GL	11/12/25 3:03:00 PM
Font color: Auto		

Page 14: [109] Formatted	GL	11/12/25 3:03:00 PM
Font color: Auto		
Page 14: [110] Formatted	GL	11/12/25 3:03:00 PM
Font color: Auto		
Page 14: [111] Formatted	GL	11/12/25 3:03:00 PM
Font color: Auto		
Page 14: [112] Formatted	GL	11/12/25 3:03:00 PM
Font color: Auto		
Page 14: [113] Formatted	GL	11/12/25 3:03:00 PM
Font color: Auto		
Page 15: [114] Deleted	GL	11/12/25 3:03:00 PM
▼		
Page 16: [115] Deleted	GL	11/12/25 3:03:00 PM
▼		
Page 17: [116] Deleted	GL	11/12/25 3:03:00 PM
▼		
Page 21: [117] Deleted	GL	11/12/25 3:03:00 PM
▼		
Page 23: [118] Deleted	GL	11/12/25 3:03:00 PM
▼		
Page 31: [119] Deleted	GL	11/12/25 3:03:00 PM
▼		
Page 33: [120] Deleted	GL	11/12/25 3:03:00 PM
▼		
Page 33: [120] Deleted	GL	11/12/25 3:03:00 PM
▼		
Page 33: [120] Deleted	GL	11/12/25 3:03:00 PM
▼		
Page 33: [120] Deleted	GL	11/12/25 3:03:00 PM
▼		
Page 33: [121] Deleted	GL	11/12/25 3:03:00 PM

Page 33: [121] Deleted GL 11/12/25 3:03:00 PM

Page 33: [122] Deleted GL 11/12/25 3:03:00 PM

Page 33: [123] Deleted GL 11/12/25 3:03:00 PM

▼

Page 33: [123] Deleted GL 11/12/25 3:03:00 PM

▼

Page 33: [124] Deleted GL 11/12/25 3:03:00 PM

▼

Page 33: [124] Deleted GL 11/12/25 3:03:00 PM

▼

Page 33: [124] Deleted GL 11/12/25 3:03:00 PM

▼

Page 33: [124] Deleted GL 11/12/25 3:03:00 PM

▼

Page 33: [125] Deleted GL 11/12/25 3:03:00 PM

▼

Page 33: [125] Deleted GL 11/12/25 3:03:00 PM

▼

Page 33: [125] Deleted GL 11/12/25 3:03:00 PM

▼

Page 33: [126] Deleted GL 11/12/25 3:03:00 PM

▼

Page 33: [126] Deleted GL 11/12/25 3:03:00 PM

▼

Page 33: [127] Deleted GL 11/12/25 3:03:00 PM

Page 33: [127] Deleted GL 11/12/25 3:03:00 PM

Page 33: [127] Deleted GL 11/12/25 3:03:00 PM

Page 33: [128] Deleted GL 11/12/25 3:03:00 PM

Page 33: [129] Deleted GL 11/12/25 3:03:00 PM

Page 38: [130] Deleted GL 11/12/25 3:03:00 PM

Page 38: [130] Deleted GL 11/12/25 3:03:00 PM

Page 38: [130] Deleted GL 11/12/25 3:03:00 PM

▼

Page 38: [130] Deleted GL 11/12/25 3:03:00 PM

▼

Page 38: [130] Deleted GL 11/12/25 3:03:00 PM

▼

Page 38: [131] Deleted GL 11/12/25 3:03:00 PM

▼

Page 38: [131] Deleted GL 11/12/25 3:03:00 PM

▼

Page 38: [131] Deleted GL 11/12/25 3:03:00 PM

▼

Page 38: [131] Deleted GL 11/12/25 3:03:00 PM

▼

Page 38: [131] Deleted GL 11/12/25 3:03:00 PM

▼

Page 38: [132] Deleted GL 11/12/25 3:03:00 PM

▼

Page 38: [132] Deleted GL 11/12/25 3:03:00 PM

▼

Page 38: [132] Deleted GL 11/12/25 3:03:00 PM

▼

Page 38: [132] Deleted GL 11/12/25 3:03:00 PM

▼

Page 38: [132] Deleted GL 11/12/25 3:03:00 PM

▼

Page 38: [133] Deleted GL 11/12/25 3:03:00 PM

Page 38: [134] Deleted GL 11/12/25 3:03:00 PM

Page 38: [135] Deleted GL 11/12/25 3:03:00 PM

▼

Page 38: [136] Deleted GL 11/12/25 3:03:00 PM

▼

Page 38: [136] Deleted GL 11/12/25 3:03:00 PM

▼

Page 38: [136] Deleted GL 11/12/25 3:03:00 PM

▼

Page 38: [136] Deleted GL 11/12/25 3:03:00 PM

▼

Page 38: [137] Deleted GL 11/12/25 3:03:00 PM

▼

Page 38: [137] Deleted GL 11/12/25 3:03:00 PM

▼

Page 38: [137] Deleted GL 11/12/25 3:03:00 PM

▼

Page 38: [137] Deleted GL 11/12/25 3:03:00 PM

▼

Page 38: [137] Deleted GL 11/12/25 3:03:00 PM

▼

Page 38: [138] Deleted GL 11/12/25 3:03:00 PM

▼

Page 38: [138] Deleted GL 11/12/25 3:03:00 PM

▼

Page 38: [138] Deleted GL 11/12/25 3:03:00 PM

▼

Page 38: [138] Deleted GL 11/12/25 3:03:00 PM

▼

Page 38: [138] Deleted GL 11/12/25 3:03:00 PM

Page 40: [139] Deleted GL 11/12/25 3:03:00 PM

Page 40: [139] Deleted GL 11/12/25 3:03:00 PM

Page 40: [139] Deleted GL 11/12/25 3:03:00 PM

Page 40: [140] Deleted GL 11/12/25 3:03:00 PM

Page 40: [141] Deleted GL 11/12/25 3:03:00 PM

Page 40: [142] Deleted GL 11/12/25 3:03:00 PM

▼

Page 40: [142] Deleted GL 11/12/25 3:03:00 PM

▼

Page 40: [143] Deleted GL 11/12/25 3:03:00 PM

▼

Page 40: [143] Deleted GL 11/12/25 3:03:00 PM

▼

Page 40: [143] Deleted GL 11/12/25 3:03:00 PM

▼

Page 40: [143] Deleted GL 11/12/25 3:03:00 PM

▼

Page 40: [143] Deleted GL 11/12/25 3:03:00 PM

▼

Page 40: [143] Deleted GL 11/12/25 3:03:00 PM

▼

Page 40: [144] Deleted GL 11/12/25 3:03:00 PM

▼

Page 40: [144] Deleted GL 11/12/25 3:03:00 PM

▼

Page 40: [144] Deleted GL 11/12/25 3:03:00 PM

▼

Page 40: [144] Deleted GL 11/12/25 3:03:00 PM

▼

Page 40: [144] Deleted GL 11/12/25 3:03:00 PM

▼

Page 40: [144] Deleted GL 11/12/25 3:03:00 PM

Page 40: [144] Deleted GL 11/12/25 3:03:00 PM

Page 40: [144] Deleted GL 11/12/25 3:03:00 PM

Page 40: [145] Deleted GL 11/12/25 3:03:00 PM

Page 40: [146] Deleted GL 11/12/25 3:03:00 PM

▼

Page 41: [147] Deleted GL 11/12/25 3:03:00 PM

▼

Page 41: [147] Deleted GL 11/12/25 3:03:00 PM

▼

Page 41: [147] Deleted GL 11/12/25 3:03:00 PM

▼

Page 41: [148] Deleted GL 11/12/25 3:03:00 PM

▼

Page 41: [148] Deleted GL 11/12/25 3:03:00 PM

▼

Page 41: [148] Deleted GL 11/12/25 3:03:00 PM

▼

Page 41: [148] Deleted GL 11/12/25 3:03:00 PM

▼

Page 41: [148] Deleted GL 11/12/25 3:03:00 PM

▼

Page 41: [149] Deleted GL 11/12/25 3:03:00 PM

▼

Page 41: [149] Deleted GL 11/12/25 3:03:00 PM

▼

Page 41: [149] Deleted GL 11/12/25 3:03:00 PM

▼

Page 41: [149] Deleted GL 11/12/25 3:03:00 PM

Page 41: [149] Deleted GL 11/12/25 3:03:00 PM

Page 41: [150] Deleted GL 11/12/25 3:03:00 PM

Page 41: [151] Deleted GL 11/12/25 3:03:00 PM

Page 41: [152] Deleted GL 11/12/25 3:03:00 PM

Page 41: [152] Deleted GL 11/12/25 3:03:00 PM

▼

Page 41: [152] Deleted GL 11/12/25 3:03:00 PM

▼

Page 41: [152] Deleted GL 11/12/25 3:03:00 PM

▼

Page 41: [152] Deleted GL 11/12/25 3:03:00 PM

▼

Page 41: [152] Deleted GL 11/12/25 3:03:00 PM

▼

Page 41: [152] Deleted GL 11/12/25 3:03:00 PM

▼

Page 41: [153] Deleted GL 11/12/25 3:03:00 PM

▼

Page 41: [153] Deleted GL 11/12/25 3:03:00 PM

▼

Page 41: [153] Deleted GL 11/12/25 3:03:00 PM

▼

Page 41: [153] Deleted GL 11/12/25 3:03:00 PM

▼

Page 41: [153] Deleted GL 11/12/25 3:03:00 PM

▼

Page 41: [153] Deleted GL 11/12/25 3:03:00 PM